



Regulation of blood pressure and renal electrolyte balance by Cullin-RING ligases

Shinichi Uchida

Purpose of review

Efforts to explore the pathogenic mechanisms underlying hereditary hypertension caused by a single gene mutation have brought about conceptual advances in our understanding of blood pressure regulation. We here discuss a novel pathogenic mechanism underlying the hereditary hypertensive disease pseudohypoaldosteronism type II (PHAII), caused by mutations in three different genes encoding for Cullin-3, Kelch-like protein 3 (KLHL3), and with-no-lysine kinases (WNKs).

Recent findings

In 2001, mutations in genes encoding for WNKs were identified as being responsible for PHAII. Recent advancements in genetics, in particular whole-exome sequencing, have revealed that mutations in two additional genes encoding for KLHL3 and Cullin3 also cause PHAII. This discovery contributed to the clarification of the previously unknown regulatory mechanism of WNKs, namely WNK ubiquitination by the KLHL3–Cullin-3 E3 ligase complex.

Summary

Levels of WNKs within cells are regulated via ubiquitination by the KLHL3–Cullin-3 E3 ligase complex and are important determinants of the activity of the WNK-oxidative stress-responsive gene 1 and Ste20-related proline-alanine-rich kinase–SLC12A transporter signaling cascade. The PHAII-causing mutations in WNK4, KLHL3, and Cullin-3 result in the decreased ubiquitination and increased abundance of WNK4 in the kidney, thereby activating the thiazide-sensitive NaCl cotransporter and causing PHAII.

Keywords

blood pressure, Cullin-3, Kelch-like protein 3, kidney, NaCl cotransporter, with-no-lysine kinase

INTRODUCTION

Hypertension is one of the biggest health problems in the industrialized world because it damages critical organs. Studies of monogenic hypertensive diseases, such as Liddle syndrome and pseudohypoaldosteronism type II (PHAII), have provided new insights into the mechanisms of blood pressure regulation in humans. PHAII is an autosomal dominant hereditary hypertensive disease characterized by hyperkalemia, metabolic acidosis, and thiazide sensitivity [1]. Genes encoding for with-no-lysine kinases (WNKs) (WNK1 and WNK4) were identified in 2001 as being responsible for PHAII [2]. Recently, two new genes encoding for Kelch-like protein 3 (KLHL3) and Cullin-3 were also identified as being responsible for PHAII [3^{***}, 4^{***}]. Therefore, determining how these causative genes (*WNK*, *KLHL3*, and *Cullin-3*) are orchestrated and how pathogenic mutations in these genes cause a common hypertensive disease would contribute to the understanding of the molecular pathogenesis of hypertension in humans and to the identification of new targets

for antihypertensive drugs. We discuss this issue on the basis of the recently published data.

PSEUDOHYPOALDOSTERONISM TYPE II AND WITH-NO-LYSINE KINASES

At the time when *WNK1* and *WNK4* were identified as the causative genes for PHAII, a substrate for WNKs was yet to be identified, but it was expected that NaCl cotransporter (NCC) was regulated by *WNK1* and *WNK4* because PHAII is a thiazide-sensitive disease.

Department of Nephrology, Graduate Schools of Medical and Dental Sciences, Tokyo Medical and Dental University, Tokyo, Japan

Correspondence to Shinichi Uchida, Department of Nephrology, Graduate Schools of Medical and Dental Sciences, Tokyo Medical and Dental University, 1–5–45 Yushima Bunkyo, Tokyo 113–8519, Japan. Tel: +81 3 5803 5214; fax: +81 3 5803 5215; e-mail: suchida.kid@tmd.ac.jp

Curr Opin Nephrol Hypertens 2014, 23:487–493

DOI:10.1097/MNH.000000000000049

KEY POINTS

- WNKs are substrates for the KLHL2/3–Cullin-3 E3 ligase complex.
- Impaired degradation of WNK4 and its subsequent increase in the kidney is the common mechanism underlying PHAI, caused by mutations in three different genes encoding for WNK4, KLHL3, and Cullin-3.
- It is important to investigate whether KLHL2/3-mediated regulations of WNKs are involved in the pathophysiology of diseases other than PHAI.

The mutations found in *WNK1* are large deletions in intron 1, which were considered to increase its transcription [2]. The mutations of *WNK4* are four missense mutations, three of which are clustered within a distance of four amino acids in a region termed the ‘acidic domain’ [2]. This acidic domain is well conserved in all WNK isoforms [5].

WITH-NO-LYSINE KINASE SIGNALING REGULATING SOLUTE CARRIER FAMILY MEMBER 12A TRANSPORTERS

After the identification of *WNK1* and *WNK4* as the causative genes for PHAI, numerous investigations of the effects of the coexpression of WNK1 and WNK4 with transporters, including NCC, were published [6–14]. However, the detailed mechanisms of this regulation, in particular the intracellular signaling cascades involved, were poorly understood. Then, the oxidative stress-responsive gene 1 (OSR1) and Ste20-related proline-alanine-rich kinase (SPAK) were identified as substrates for WNK1 and WNK4 [15,16]. OSR1 and SPAK are related Ser–Thr kinases that belong to the Ste20 kinase subfamily [5], and were already identified as regulators of the SLC12A2 [also known as Na–K–2Cl–cotransporter 1 (NKCC1)] cotransporter [17–20]. Therefore, SLC12A3 (also known as NCC) and SLC12A1 [also known as Na–K–2Cl–cotransporter 2 (NKCC2)], which belong to the same transporter family as NKCC1, could also act as substrates for OSR1 and SPAK. To prove this, and to clarify the molecular pathogenesis of PHAI in the kidney *in vivo*, Yang *et al.* [21] generated a mouse model of PHAI, that is, a knock-in mouse carrying a PHAI-causing missense mutation in *WNK4* (D561A), corresponding to the D564A mutation in patients with PHAI. At the same time, they generated anti-phosphorylated NCC (pNCC) antibodies that recognized potential Ser and Thr phosphorylation sites by OSR1 and SPAK, deduced from sequence alignment with NKCC1. Using the anti-pNCC antibodies, Yang *et al.* [21] demonstrated that NCC phosphorylation was

significantly increased in the kidneys of PHAI model mice and that pNCC was concentrated on the apical plasma membranes of the distal convoluted tubules. SPAK and OSR1 phosphorylation at the specific phosphorylation sites by WNK was also increased in *Wnk^{D561A/+}* mice, suggesting that WNK–OSR1/SPAK–NCC signaling was present in the kidney and was activated by the PHAI-causing *WNK4* mutation. The WNK responsible for NCC phosphorylation in the kidney was later identified as WNK4 through the analysis of *WNK1*, *WNK3*, and *WNK4* knockout mice [22–24,25].

The mechanism of NCC activation by phosphorylation may be mainly mediated by increased NCC accumulation in the apical plasma membranes of the distal convoluted tubules [21,26,27]. Hossain Khan *et al.* [28] found that phosphorylation of NCC decreased its ubiquitination, and decreased endocytosis and degradation may underlie the increased accumulation of phosphorylated NCC evident in the apical plasma membranes of the distal convoluted tubules.

Apart from NCC regulation, WNK signaling is involved in NKCC1 and NKCC2 regulation. NKCC2 is a target of furosemide and is present on the apical plasma membranes in the thick ascending limb of Henle’s loop (TAL). Lin *et al.* [29] generated kidney-specific OSR1 knockout mice, which showed Batter syndrome-like phenotypes with reduced NKCC2 phosphorylation. These data indicate the existence of OSR1–NKCC2 signaling in TAL, although the responsible WNK-regulating OSR1 in TAL remains to be determined (Fig. 1). WNK4 may not be the one as no reduction in NKCC2 phosphorylation was observed in *WNK4* knockout mice (unpublished observation).

In SPAK knockout mice, in addition to the decreased NCC phosphorylation in the kidney, NKCC1 phosphorylation was decreased in the aorta, which showed decreased contractility after phenylephrine administration. Recently, Zeniya *et al.* [30] reported that WNK3 was the WNK responsible for this signaling in the aorta and that this WNK3–SPAK–NKCC1 cascade was regulated by angiotensin II. Thus, WNK may be significantly contributing to blood pressure regulation in extrarenal tissues and the kidney.

NEW GENES CAUSATIVE FOR PSEUDOHYPOALDOSTERONISM TYPE II

Recently, two new genes, *KLHL3* and *Cullin-3*, were identified as being responsible for causing PHAI [3^{••},4^{••}]. Cullin-3 is one of the six cullins identified in eukaryotes, and cullin-3-based Cullin-RING ubiquitin ligases (CRLs) have been recently identified as being involved in developmental and stress

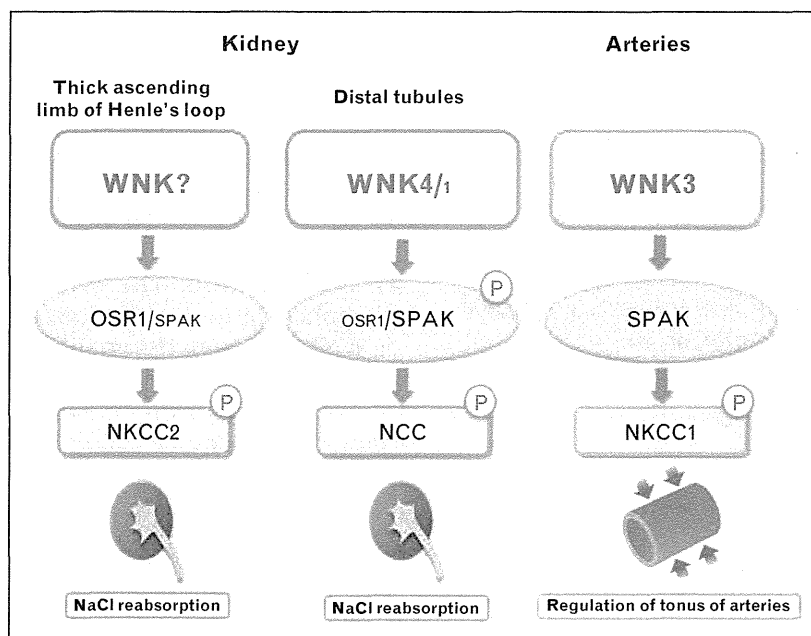


FIGURE 1. WNK signaling in kidneys and arteries. In the signal cascades of WNK–OSR1/SPAK–SLC12A transporters, WNK4 and SPAK may play a dominant role in NCC (SLC12A3) phosphorylation. Likewise, WNK3 (possibly also WNK1) and SPAK (possibly also OSR1) may have similar roles in NKCC1 phosphorylation (SLC12A2) in the smooth muscle cells of arteries. OSR1 was shown to have a major role in NKCC2 (SLC12A1) phosphorylation. The upstream WNK regulating OSR1 in TAL remains to be determined. WNK4 may not be the one as no reduction in NKCC2 phosphorylation was observed in WNK4 knockout mice (unpublished observation).

responses, as well as human hereditary diseases [31^o]. Ubiquitin ligase, also known as E3 ligase, is a key element in the ubiquitin or proteasome system that transfers ubiquitin moieties to substrates. Among several hundreds of E3 ligases identified to date, CRLs constitute the most prevalent class of E3. As shown in Fig. 2, Cullin-3 serves as a scaffold for

the catalytic module of a RING finger protein (Rbx1) and a ubiquitin-conjugating enzyme (E2), and a substrate adaptor module. Cullin-3 binds to several substrate adaptor proteins that have BTB domains. The name BTB is derived from a homologous, 115-amino acid domain present in *Drosophila melanogaster* *bric a brac 1*, *tramtrack*, and *broad complex*

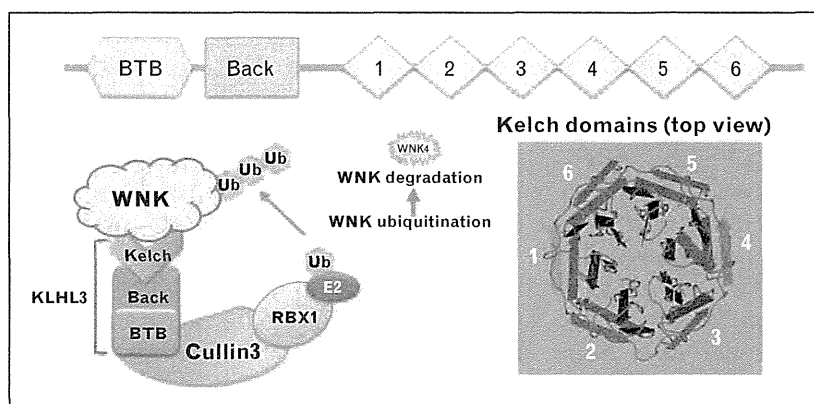


FIGURE 2. Primary and three-dimensional structures of a KLHL protein and its function as a component of CRL3. Upper panel: the primary structure of Kelch-like (KLHL) proteins with N-terminal BTB and BACK domains and five to six C-terminal Kelch domains. The BTB domain is a binding site for Cullin 3, and Kelch repeats constitute a propeller structure, as shown in the right lower panels, to capture a substrate. Each Kelch domain forms a blade, and most PHAII-causing mutations (shown in yellow lines) are located in the loop regions linking each blade, which may be involved in substrate binding. Left lower panel: KLHL3 and Cullin-3 forms an E3 ligase complex with the RING finger protein, RBX1. WNKs are captured by this E3 ligase by binding to KLHL3 and are ubiquitinated and degraded.

proteins that facilitates protein–protein interaction [32]. Several substrate-binding domains, such as Kelch, WD40, and basic leucine zipper, are commonly found in the BTB domain-containing adaptor proteins in CRL3.

The Kelch-like protein family consists of more than 40 members [33]. In general, KLHL proteins contain one BTB domain, one BTB and C-terminal Kelch (BACK) domain, and five to six Kelch domains (Fig. 2). The Kelch domain forms one blade of a β-propeller structure, which is also involved in the protein–protein interaction. Kelch domain-containing proteins have been shown to participate in many cellular functions [34] because substrates for KLHL–CUL3 E3 ligases are diverse. A list of the functions of KLHL–CUL3 E3 ligases and their involvement in disease is presented in Table 1 [3^{••},4^{••},35,36^{••},37^{••},38–56].

PATHOGENESIS OF PSEUDOHYPOALDOSTERONISM TYPE II THROUGH MUTATIONS IN THREE DIFFERENT GENES

As mutations in *WNK4*, *KLHL3*, and *Cullin-3* cause the same disease, PHAI, it is reasonable to speculate

that components of WNK–OSR1/SPAK–NCC signaling cascade, in particular WNK4, could be the substrate for the KLHL3–Cullin-3 E3 ligase complex. In fact, Ohta *et al.* [36^{••}] and Wakabayashi *et al.* [37^{••}] reported that WNK1 and WNK4 were substrates for the KLHL3–Cullin-3 E3 ligase complex, respectively. Then, two further reports [57[•],58[•]] demonstrated WNK4 as a target of the KLHL3–Cullin-3 E3 ligase complex. Analyses of PHAI-causing mutations in *WNK4*, *KLHL3*, and *Cullin-3* also confirmed this notion. Wakabayashi *et al.* [37^{••}] and Mori *et al.* [59] showed that binding of KLHL3 to WNK4 was abolished by PHAI-causing mutations in *WNK4*, indicating that the acidic domain is involved in the binding to KLHL3. In contrast to WNK4, mutations in *KLHL3* were not clustered to a single domain, but were present in the BTB, BACK, and Kelch domains. Mutations in the BTB and BACK domains affected the ability of KLHL3 to bind Cullin-3, whereas mutations in the Kelch domains affected the ability of KLHL3 to bind WNK1 and WNK4 [59]. Thus, impaired binding of KLHL3 to Cullin-3 or WNK4 decreased WNK4 ubiquitination, resulting in increased WNK4 proteins within cells.

Almost all PHAI-causing *Cullin-3* mutations are found around the splice donor and acceptor sites of

Table 1. List of KLHL–CUL3 E3s: functions and involvement in disease

Name	Substrate	Function	Disease	Reference
KLHL2	WNK	ND	ND	[35]
KLHL3	WNK1	Regulation of SLC12A transporters	PHAI	[3 ^{••} ,4 ^{••} ,36 ^{••} ,37 ^{••}]
	WNK4	ND	ND	
KLHL7	ND	ND	adRP	[38]
KLHL8	Rapsyn	AChR clustering	ND	[39]
KLHL9	AuroraB	Mitosis	Distal myopathy	[40,41]
KLHL13	ND	ND	ND	[42]
KLHL21	ND	ND	ND	[43]
KLHL12	Disheveled	Wnt/β-catenin signaling	ND	[44]
	Sec31	Collagen secretion	ND	[45]
KLHL16/Gigaxonin	MAP1B	Regulation of cytoskeletal proteins	Giant axonal neuropathy	[46]
	Intermediate filaments	ND	ND	[47]
KLHL19/Keap1	Nrf2	Oxidative stress response	Cancer	[48]
				[49]
				[50]
				[51]
KLHL20	PML	HIF-1 signaling	Progression of prostate cancer	[52]
	DAPK	INF-induced response	ND	[53]
	PLK1	Chromosome segregation	ND	[54]
KLHL22	PLK1	Chromosome segregation	ND	[55]
KLHL25	4E-BP	Translational regulation	ND	[56]

AChR, acetylcholine receptor; adRP, autosomal dominant retinitis pigmentosa; DAPK, death-associated protein kinase; ND, not determined; Nrf2, NF-E2-related factor 2; PHAI, pseudohypoaldosteronism type II; PLK1: polo-like kinase 1; PML, promyelocytic leukemia; WNK, with-no-lysine kinase.

exon 9. Osawa *et al.* [60] and Tsuji *et al.* [61] recently verified that exon 9 was skipped in the leukocytes of patients with PHAII-causing *Cullin-3* mutations, as shown by the experiment in cultured cells by Boyden *et al.* [37^{***}]. Overexpression of the mutant *Cullin-3* lacking a portion of exon 9 with KLHL3 showed less ability to reduce the coexpressed WNK4 [37^{***}], suggesting that the mutant *Cullin-3* may have less E3 ligase activity. Thus, all PHAII-causing mutations in *WNK4*, *KLHL3*, and *Cullin-3* resulted in a common consequence, that is, decreased WNK4 ubiquitination and increased WNK4 protein within cells (Fig. 3).

This increase in WNK4 protein was confirmed in the kidneys of *Wnk^{4DS61A/+}* mice [37^{***}]. Because WNK4, as well as WNK1, was shown to phosphorylate and activate OSR1 and SPAK *in vitro* [15], the increase in WNK4 must be stimulatory to downstream WNK–OSR1/SPAK–NCC signaling. However,

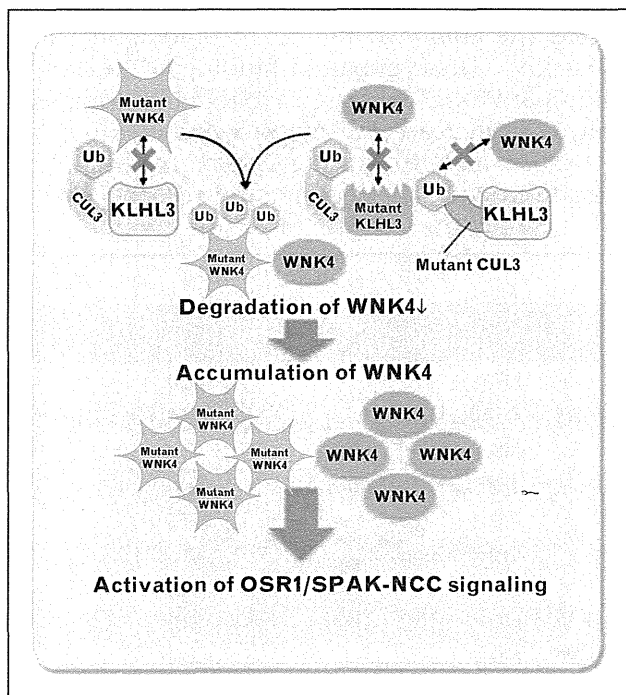


FIGURE 3. Molecular pathogenesis of PHAII. Under normal conditions, WNK 4 proteins within cells are maintained by appropriate degradation after ubiquitination by the KLHL3–Cullin-3 E3 ligase complex. However, PHAII-causing mutations in the acidic domain of WNK4 and in the Kelch domains of KLHL3 affect their binding, thereby reducing the ubiquitination and degradation of WNK4. PHAII-causing mutant *Cullin-3* lacking the portion corresponding to exon 9 is less able to decrease WNK4, probably because of its reduced E3 ligase activity. Thus, PHAII-causing mutations in the three different genes have a common consequence, that is, decreased WNK4 ubiquitination and increased WNK4 protein levels within DCT, leading to the activation of OSR1/SPAK–NCC signaling and to PHAII.

long-standing controversy exists over the influence of WNK4 on NCC function [62]. Initially, WNK4 overexpression experiments in *Xenopus laevis* oocytes showed that WNK4 is a negative regulator of NCC [6,7]. However, Castaneda-Bueno *et al.* [25^{***}] reported that *WNK4* knockout mice exhibit a phenotype reminiscent of Gitelman syndrome (Gitelman syndrome is caused by the loss of function of NCC), indicating that WNK4 is a positive regulator of NCC *in vivo*. Moreover, WNK4 transgenic mice showed robust increases in OSR1, SPAK, and NCC phosphorylation and showed phenotypes similar to PHAII [37^{***}]. Therefore, it is now clear that increased wild-type WNK4 in the kidney activates the WNK–OSR1/SPAK–NCC signaling cascade and causes PHAII. Thus, the long-standing controversy about the influence of WNK4 on NCC was settled by the discovery of the two new causative genes for PHAII. This controversial story gives us an important lesson that it is very risky to make conclusions based on results from a single experimental system, especially from *in-vitro* overexpression studies. In this regard, the scheme depicted in Fig. 3 should also be validated in mouse models carrying the PHAII-causing mutations in *KLHL3* or *Cullin-3*.

UNANSWERED QUESTIONS AND FUTURE PERSPECTIVES

Thus, impaired ubiquitination and a consequent increase in WNK4 protein were established as the molecular pathogenesis of PHAII, caused by mutations in *WNK4*, *KLHL3*, and *Cullin-3* (Fig. 3). There are several questions to be answered in future. First, is WNK4 the only WNK regulated by the KLHL3–Cullin-3 E3 ligase complex in the kidney *in vivo*? In fact, *in-vitro* experiments clearly show that both WNK1 and WNK4 proteins were regulated by the KLHL3–Cullin-3 E3 ligase complex [36^{***},37^{***}]. Therefore, levels of both WNK1 and WNK4 may be increased in the kidneys of patients with PHAII carrying mutations in *KLHL3* and *Cullin-3*, further contributing to the activation of WNK–OSR1/SPAK–NCC signaling and explaining the more severe PHAII phenotypes evident with mutations in *Cullin-3* and *KLHL3* than in *WNK1* and *WNK4* [37^{***}]. Moreover, other WNKs, such as WNK2 and WNK3, could be substrates for the KLHL3–Cullin-3 E3 ligase complex because the KLHL3-binding domain of WNK4 (the acidic domain) is highly conserved in all WNK isoforms. Furthermore, KLHL2, the closest homolog to KLHL3 among KLHL proteins, was shown to behave similarly to KLHL3 in terms of E3 ligase for WNKs [35]. These data suggest that both KLHL2 and KLHL3 may be involved in the regulation of all WNKs in various types of cells. It would also be interesting to confirm

whether there are regulatory mechanisms controlling the interaction between KLHL2/3 and WNKs. Although several regulations of WNKs by diets and hormonal factors have been reported, the detailed mechanisms are largely unknown. Regulated binding of KLHL2/3 and WNKs by phosphorylation or other modifications may be one of the important mechanisms of WNK regulation. Finally, one of the biggest questions may be why mutation in Cullin-3, which is ubiquitously expressed and functions as a scaffold of E3 not only for KLHL3 but also for many other adaptor proteins, induces the kidney-specific disease PHAI. The skipping of exon 9 might occur dominantly in DCT cells in the kidney; however, we can also confirm the skipping in the white blood cells of the patients. Another possibility would be that the mutant Cullin-3 might be functionally defective as E3 ligase only with KLHL3. A knock-in mouse model carrying the same mutations in *Cullin-3* is necessary to answer these questions.

CONCLUSION

Why PHAI-causing missense mutations in *WNK4* are clustered and how these mutations activate downstream signaling to NCC has been a long-standing unanswered question. The recent discovery of two additional genes causing PHAI helped construct a complete picture of the molecular pathogenesis of PHAI and provided definite genetic evidence that *WNK4* in the kidney never behaves as a negative regulator of NCC but acts as a positive regulator through *WNK-OSR1/SPAK-NCC* signaling. Levels of WNKs within cells, regulated via ubiquitination by *KLHL2/3-Cullin-3 E3* ligases, would be important determinants of the activity of the WNK signaling cascade.

Acknowledgements

This study was supported in part by Grants-in-Aid for Scientific Research (S) from the Japan Society for the Promotion of Science, the Ministry of Health Labor and Welfare (a Health Labor Science Research Grant), Salt Science Research Foundation (No. 1026, 1228), and the Takeda Science Foundation.

Conflicts of interest

There are no conflicts of interest.

REFERENCES AND RECOMMENDED READING

Papers of particular interest, published within the annual period of review, have been highlighted as:

- of special interest
- of outstanding interest

1. Gordon RD. Syndrome of hypertension and hyperkalemia with normal glomerular filtration rate. *Hypertension* 1986; 8:93–102.
2. Wilson FH, Disse-Nicodème S, Choate KA, *et al.* Human hypertension caused by mutations in *WNK* kinases. *Science* 2001; 293:1107–1112.
3. Boyden LM, Choi M, Choate KA, *et al.* Mutations in kelch-like 3 and cullin 3 cause hypertension and electrolyte abnormalities. *Nature* 2012; 482:98–102.
4. Exome-sequencing discovered *KLHL3* and *Cullin-3* as the new genes causative for PHAI.
5. Louis-Dit-Picard H, Barc J, Trujillo D, *et al.* *KLHL3* mutations cause familial hyperkalemic hypertension by impairing ion transport in the distal nephron. *Nat Genet* 2012; 44:456–460.
6. Exome-sequencing discovered *KLHL3* as a new gene causative for PHAI.
7. Richardson C, Alessi DR. The regulation of salt transport and blood pressure by the *WNK-SPAK/OSR1* signalling pathway. *J Cell Sci* 2008; 121:3293–3304.
8. Wilson FH, Kahle KT, Sabath E, *et al.* Molecular pathogenesis of inherited hypertension with hyperkalemia: the Na-Cl cotransporter is inhibited by wild-type but not mutant *WNK4*. *Proc Natl Acad Sci U S A* 2003; 100:680–684.
9. Yang CL, Angell J, Mitchell R, *et al.* *WNK* kinases regulate thiazide-sensitive Na-Cl cotransport. *J Clin Invest* 2003; 111:1039–1045.
10. Kahle KT, Wilson FH, Leng Q, *et al.* *WNK4* regulates the balance between renal NaCl reabsorption and K⁺ secretion. *Nat Genet* 2003; 35:372–376.
11. Yamauchi K, Rai T, Kobayashi K, *et al.* Disease-causing mutant *WNK4* increases paracellular chloride permeability and phosphorylates claudins. *Proc Natl Acad Sci U S A* 2004; 101:4690–4694.
12. Yamauchi K, Yang SS, Ohta A, *et al.* Apical localization of renal K channel was not altered in mutant *WNK4* transgenic mice. *Biochem Biophys Res Commun* 2005; 332:750–755.
13. Gamba G. TRPV4: a new target for the hypertension-related kinases *WNK1* and *WNK4*. *Am J Physiol Renal Physiol* 2006; 290:F1303–1304.
14. Garzon-Muvdi T, Pacheco-Alvarez D, Gagnon KB, *et al.* *WNK4* kinase is a negative regulator of K⁺-Cl⁻ cotransporters. *Am J Physiol Renal Physiol* 2007; 292:F1197–1207.
15. Ring AM, Cheng SX, Leng Q, *et al.* *WNK4* regulates activity of the epithelial Na⁺ channel *in vitro* and *in vivo*. *Proc Natl Acad Sci U S A* 2007; 104:4020–4024.
16. Yang CL, Liu X, Paliege A, *et al.* *WNK1* and *WNK4* modulate CFTR activity. *Biochem Biophys Res Commun* 2007; 353:535–540.
17. Moriguchi T, Urushiyama S, Hisamoto N, *et al.* *WNK1* regulates phosphorylation of cation-chloride-coupled cotransporters via the STE20-related kinases, *SPAK* and *OSR1*. *J Biol Chem* 2005; 280:42685–42693.
18. Vitari AC, Deak M, Morrice NA, *et al.* The *WNK1* and *WNK4* protein kinases that are mutated in Gordon's hypertension syndrome phosphorylate and activate *SPAK* and *OSR1* protein kinases. *Biochem J* 2005; 391:17–24.
19. Flemmer AW, Gimenez I, Dowd BF, *et al.* Activation of the Na-K-Cl cotransporter *NKCC1* detected with a phospho-specific antibody. *J Biol Chem* 2002; 277:37551–37558.
20. Piechotta K, Lu J, Delpire E. Cation chloride cotransporters interact with the stress-related kinases Ste20-related proline-alanine-rich kinase (*SPAK*) and oxidative stress response 1 (*OSR1*). *J Biol Chem* 2002; 277:50812–50819.
21. Dowd BF, Forbush B. *PASK* (proline-alanine-rich STE20-related kinase), a regulatory kinase of the Na-K-Cl cotransporter (*NKCC1*). *J Biol Chem* 2003; 278:27347–27353.
22. Piechotta K, Garbarini N, England R, *et al.* Characterization of the interaction of the stress kinase *SPAK* with the Na⁺-K⁺-2Cl⁻ cotransporter in the nervous system: evidence for a scaffolding role of the kinase. *J Biol Chem* 2003; 278:52848–52856.
23. Yang SS, Morimoto T, Rai T, *et al.* Molecular pathogenesis of pseudohypoaldosteronism type II: generation and analysis of a *Wnk4*^(D561A/I) knockin mouse model. *Cell Metab* 2007; 5:331–344.
24. Ohta A, Rai T, Yui N, *et al.* Targeted disruption of the *Wnk4* gene decreases phosphorylation of Na-Cl cotransporter, increases Na excretion and lowers blood pressure. *Hum Mol Genet* 2009; 18:3978–3986.
25. Susa K, Kita S, Iwamoto T, *et al.* Effect of heterozygous deletion of *WNK1* on the *WNK-OSR1/SPAK-NCC/NKCC1/NKCC2* signal cascade in the kidney and blood vessels. *Clin Exp Nephrol* 2012; 16:530–538.
26. Oi K, Sahara E, Rai T, *et al.* A minor role of *WNK3* in regulating phosphorylation of renal *NKCC2* and *NCC* co-transporters *in vivo*. *Biol Open* 2012; 1:120–127.
27. Castaneda-Bueno M, Cervantes-Perez LG, Vazquez N, *et al.* Activation of the renal Na⁺-Cl⁻ cotransporter by angiotensin II is a *WNK4*-dependent process. *Proc Natl Acad Sci U S A* 2012; 109:7929–7934.
28. *WNK4* knockout mice showed phenotypes similar to Gitelman's syndrome, clearly indicating that *WNK4* is a positive regulator of *NCC*.
29. Pedersen NB, Hofmeister MV, Rosenbaek LL, *et al.* Vasopressin induces phosphorylation of the thiazide-sensitive sodium chloride cotransporter in the distal convoluted tubule. *Kidney Int* 2010; 78:160–169.
30. Lee DH, Maunsbach AB, Riquier-Brisson AD, *et al.* Effects of ACE inhibition and ANG II stimulation on renal Na-Cl cotransporter distribution, phosphorylation, and membrane complex properties. *Am J Physiol Cell Physiol* 2013; 304:C147–163.
31. Hossain Khan MZ, Sahara E, Ohta A, *et al.* Phosphorylation of Na-Cl cotransporter by *OSR1* and *SPAK* kinases regulates its ubiquitination. *Biochem Biophys Res Commun* 2012; 425:456–461.

29. Lin SH, Yu IS, Jiang ST, *et al.* Impaired phosphorylation of Na(+)-K(+)-2Cl(-) cotransporter by oxidative stress-responsive kinase-1 deficiency manifests hypotension and Bartter-like syndrome. *Proc Natl Acad Sci U S A* 2011; 108:17538–17543.
30. Zeniya M, Sohara E, Kita S, *et al.* Dietary salt intake regulates WNK3-SPAK-NKCC1 phosphorylation cascade in mouse aorta through angiotensin II. *Hypertension* 2013; 62:872–878.
31. Genschik P, Sumara I, Lechner E. The emerging family of CULLIN3-RING ubiquitin ligases (CRL3s): cellular functions and disease implications. *EMBO J* 2013; 32:2307–2320.
- A recent review on Cullin-3-RING ubiquitin ligase proving its involvement in human pathophysiological conditions.
32. Zollman S, Godt D, Prive GG, *et al.* The BTB domain, found primarily in zinc finger proteins, defines an evolutionarily conserved family that includes several developmentally regulated genes in *Drosophila*. *Proc Natl Acad Sci U S A* 1994; 91:10717–10721.
33. Dhanoa BS, Cogliati T, Satish AG, *et al.* Update on the Kelch-like (KLHL) gene family. *Hum Genomics* 2013; 7:13.
- A recent comprehensive review of KLHL proteins.
34. Adams J, Kelso R, Cooley L. The kelch repeat superfamily of proteins: propellers of cell function. *Trends Cell Biol* 2000; 10:17–24.
35. Takahashi D, Mori T, Wakabayashi M, *et al.* KLHL2 interacts with and ubiquitinates WNK kinases. *Biochem Biophys Res Commun* 2013; 437:457–462.
36. Ohta A, Schumacher FR, Mehellou Y, *et al.* The CUL3-KLHL3 E3 ligase complex mutated in Gordon's hypertension syndrome interacts with and ubiquitylates WNK isoforms: disease-causing mutations in KLHL3 and WNK4 disrupt interaction. *Biochem J* 2013; 451:111–122.
- WNK1 was identified to be ubiquitinated by CUL3-KLHL3 E3 ligase. PHAI1-causing mutations in WNK4 were shown to decrease the binding between WNK4 and KLHL3, but WNK4 ubiquitination by CUL3-KLHL3 E3 ligase was not shown.
37. Wakabayashi M, Mori T, Isobe K, *et al.* Impaired KLHL3-mediated ubiquitination of WNK4 causes human hypertension. *Cell Rep* 2013; 3:858–868.
- WNK4 was identified to be ubiquitinated by CUL3-KLHL3 E3 ligase, and PHAI1-causing mutations in WNK4, KLHL3, and Cullin-3 were shown to result in the decreased ubiquitination and increased abundance of WNK4 within cells. In the studies of wild-type WNK4 transgenic mice, the increase in WNK4 in the kidney was clearly shown to activate NCC by phosphorylation and to induce PHAI1 phenotypes.
38. Kigoshi Y, Tsuruta F, Chiba T. Ubiquitin ligase activity of Cul3-KLHL7 protein is attenuated by autosomal dominant retinitis pigmentosa causative mutation. *J Biol Chem* 2011; 286:33613–33621.
39. Nam S, Min K, Hwang H, *et al.* Control of rapsyn stability by the CUL-3-containing E3 ligase complex. *J Biol Chem* 2009; 284:8195–8206.
40. Sumara I, Quadroni M, Frei C, *et al.* A Cul3-based E3 ligase removes Aurora B from mitotic chromosomes, regulating mitotic progression and completion of cytokinesis in human cells. *Dev Cell* 2007; 12:887–900.
41. Sumara I, Peter M. A Cul3-based E3 ligase regulates mitosis and is required to maintain the spindle assembly checkpoint in human cells. *Cell Cycle* 2007; 6:3004–3010.
42. Cirak S, von Deimling F, Sachdev S, *et al.* Kelch-like homologue 9 mutation is associated with an early onset autosomal dominant distal myopathy. *Brain* 2010; 133:2123–2135.
43. Maerki S, Olma MH, Staubli T, *et al.* The Cul3-KLHL21 E3 ubiquitin ligase targets, aurora B to midzone microtubules in anaphase and is required for cytokinesis. *J Cell, Biol* 2009; 187:791–800.
44. Angers S, Thorpe CJ, Biechele TL, *et al.* The KLHL12-Cullin-3 ubiquitin ligase negatively regulates the Wnt-beta-catenin pathway by targeting dishevelled for degradation. *Nature Cell Biol* 2006; 8:348–357.
45. Jin L, Pahuja KB, Wickliffe KE, *et al.* Ubiquitin-dependent regulation of COPII coat size and function. *Nature* 2012; 482:495–500.
46. Allen E, Ding J, Wang W, *et al.* Gigaxonin-controlled degradation of MAP1B light chain is critical to neuronal survival. *Nature* 2005; 438:224–228.
47. Bomont P, Cavalier L, Blondeau F, *et al.* The gene encoding gigaxonin, a new member of the cytoskeletal BTB/kelch repeat family, is mutated in giant axonal neuropathy. *Nat Genet* 2000; 26:370–374.
48. Mahammad S, Murthy SN, Didonna A, *et al.* Giant axonal neuropathy-associated gigaxonin mutations impair intermediate filament protein degradation. *J Clin Invest* 2013; 123:1964–1975.
49. Cullinan SB, Gordan JD, Jin J, *et al.* The Keap1-BTB protein is an adaptor that bridges Nrf2 to a Cul3-based E3 ligase: oxidative stress sensing by a Cul3-Keap1 ligase. *Mol Cell Biol* 2004; 24:8477–8486.
50. Kobayashi A, Kang MI, Okawa H, *et al.* Oxidative stress sensor Keap1 functions as an adaptor for Cul3-based E3 ligase to regulate proteasomal degradation of Nrf2. *Mol Cell Biol* 2004; 24:7130–7139.
51. Zhang DD, Lo SC, Cross JV, *et al.* Keap1 is a redox-regulated substrate adaptor protein for a Cul3-dependent ubiquitin ligase complex. *Mol Cell Biol* 2004; 24:10941–10953.
52. Padmanabhan B, Tong KI, Ohta T, *et al.* Structural basis for defects of Keap1 activity provoked by its point mutations in lung cancer. *Mol Cell* 2006; 21:689–700.
53. Yuan WC, Lee YR, Huang SF, *et al.* A Cullin3-KLHL20 Ubiquitin ligase-dependent pathway targets PML to potentiate HIF-1 signaling and prostate cancer progression. *Cancer Cell* 2011; 20:214–228.
54. Lee YR, Yuan WC, Ho HC, *et al.* The Cullin 3 substrate adaptor KLHL20 mediates DAPK ubiquitination to control interferon responses. *EMBO J* 2010; 29:1748–1761.
55. Beck J, Peter M. Regulating PLK1 dynamics by Cullin3/KLHL22-mediated ubiquitylation. *Cell Cycle* 2013; 12:2528–2529.
56. Yanagiya A, Suyama E, Adachi H, *et al.* Translational homeostasis via the mRNA cap-binding protein, eIF4E. *Mol Cell* 2012; 46:847–858.
57. Shibata S, Zhang J, Puthumana J, *et al.* Kelch-like 3 and Cullin 3 regulate electrolyte homeostasis via ubiquitination and degradation of WNK4. *Proc Natl Acad Sci U S A* 2013; 110:7838–7843.
- WNK4 was identified as binding to KLHL3 and ubiquitinated as already reported by Wakabayashi *et al.* Although inhibition of the ROMK channel by WNK4 was shown to be abrogated by coexpressed KLHL3, there was no mention of how the increase in WNK4 results in NCC activation.
58. Wu G, Peng JB. Disease-causing mutations in KLHL3 impair its effect on WNK4 degradation. *FEBS Lett* 2013; 587:1717–1722.
- In the *Xenopus* oocytes system, WNK4 was also shown to be ubiquitinated and degraded by coexpressed wild-type KLHL3 but not by PHAI1-causing KLHL3s.
59. Mori Y, Wakabayashi M, Mori T, *et al.* Decrease of WNK4 ubiquitination by disease-causing mutations of KLHL3 through different molecular mechanisms. *Biochem Biophys Res Commun* 2013; 439:30–34.
60. Osawa M, Ogura Y, Isobe K, *et al.* CUL3 gene analysis enables early intervention for pediatric pseudohypoadosteronism type II in infancy. *Pediatr Nephrol* 2013; 28:1881–1884.
61. Tsuji S, Yamashita M, Unishi G, *et al.* A young child with pseudohypoadosteronism type II by a mutation of Cullin 3. *BMC Nephrol* 2013; 14:166.
62. McCormick JA, Ellison DH. The WNKs: atypical protein kinases with pleiotropic actions. *Physiol Rev* 2011; 91:177–219.

Discovery of Novel SPAK Inhibitors That Block WNK Kinase Signaling to Cation Chloride Transporters

Eriko Kikuchi,* Takayasu Mori,* Moko Zeniya,* Kiyoshi Isobe,* Mari Ishigami-Yuasa,[†] Shinya Fujii,[‡] Hiroyuki Kagechika,^{†‡} Tomoaki Ishihara,[§] Tohru Mizushima,[§] Sei Sasaki,* Eisei Soharu,* Tatemitsu Rai,* and Shinichi Uchida*

*Department of Nephrology, Graduate School of Medical and Dental Sciences, [†]Chemical Biology Screening Center, and [‡]Institute of Biomaterials and Bioengineering, Tokyo Medical and Dental University, Tokyo, Japan; and [§]Department of Analytical Chemistry, Faculty of Pharmacy, Keio University, Tokyo, Japan

ABSTRACT

Upon activation by with-no-lysine kinases, STE20/SPS1-related proline–alanine-rich protein kinase (SPAK) phosphorylates and activates SLC12A transporters such as the Na⁺-Cl⁻ cotransporter (NCC) and Na⁺-K⁺-2Cl⁻ cotransporter type 1 (NKCC1) and type 2 (NKCC2); these transporters have important roles in regulating BP through NaCl reabsorption and vasoconstriction. SPAK knockout mice are viable and display hypotension with decreased activity (phosphorylation) of NCC and NKCC1 in the kidneys and aorta, respectively. Therefore, agents that inhibit SPAK activity could be a new class of antihypertensive drugs with dual actions (*i.e.*, NaCl diuresis and vasodilation). In this study, we developed a new ELISA-based screening system to find novel SPAK inhibitors and screened >20,000 small-molecule compounds. Furthermore, we used a drug repositioning strategy to identify existing drugs that inhibit SPAK activity. As a result, we discovered one small-molecule compound (Stock 1S-14279) and an antiparasitic agent (Closantel) that inhibited SPAK-regulated phosphorylation and activation of NCC and NKCC1 *in vitro* and in mice. Notably, these compounds had structural similarity and inhibited SPAK in an ATP-insensitive manner. We propose that the two compounds found in this study may have great potential as novel antihypertensive drugs.

J Am Soc Nephrol 26: ●●●–●●●, 2014. doi: 10.1681/ASN.2014060560

Hypertension is one of the most important health problems worldwide because it may cause heart attack and stroke, which occur frequently at present. New insight into the mechanisms of BP regulation was recently provided by studies on monogenic hypertensive diseases such as Liddle's syndrome and pseudohypoaldosteronism type II (PHAII).^{1,2} PHAII is an autosomal dominant disease characterized by hypertension, hyperkalemia, and metabolic acidosis. With-no-lysine kinase WNK1 and WNK4 mutations were identified as the genes responsible for PHAII.³ We previously generated PHAII model mice (the Wnk4^{D561A/+} knock-in mouse) that carried the same mutation as patients with PHAII and discovered that the constitutive activation of the WNK-Oxidative stress-responsive 1 (OSR1) and STE20/SPS1-related proline–alanine-rich protein kinase (SPAK)-NaCl cotransporter (NCC) signal cascade is the major pathogenic mechanism of

PHAII.^{4,5} The increased phosphorylation and activation of NCC induces excessive NaCl reabsorption in the kidney and causes salt-sensitive hypertension. OSR1/SPAK kinases phosphorylate and activate not only NCC but also other Slc12a transporters such as Na⁺-K⁺-2Cl⁻ cotransporter type 1 (NKCC1) and type 2 (NKCC2).⁶ Recent studies demonstrated the notion that WNK-OSR1/SPAK-NKCC1 phosphorylation and activation in vascular smooth muscle cells

Received June 10, 2014. Accepted September 20, 2014.

Published online ahead of print. Publication date available at www.jasn.org.

Correspondence: Dr. Shinichi Uchida, Department of Nephrology, Graduate School of Medical and Dental Sciences, Tokyo Medical and Dental University, 1-5-45 Yushima, Bunkyo-ku, Tokyo 113-8519, Japan. Email: suchida.kid@tmd.ac.jp

Copyright © 2014 by the American Society of Nephrology

can play a pivotal role in the regulation of vascular tonus.^{7–10} Moreover, WNK signaling is positively controlled by aldosterone, angiotensin II, and insulin, which may contribute to hypertension in patients with hyperaldosteronism and hyperinsulinemia.^{11–15} Therefore, drugs that inhibit this signal cascade are expected to treat hypertension through dual actions (*i.e.*, NaCl diuresis and vasodilation), and may be particularly effective in patients with hyperaldosteronism or hyperinsulinemia. In this study, we focused on the SPAK kinase because SPAK knockout mice were not fatal and displayed hypotension with low NCC and NKCC1 phosphorylation in mouse kidney and aorta, respectively.^{16,17} The purposes of this study were to develop a new high-throughput screening system using ELISA and to discover novel SPAK inhibitors from libraries of small-molecule compounds and existing drugs.

RESULTS

Development of an ELISA System for the Detection of SPAK-Regulated NKCC2 Phosphorylation

To find novel inhibitors of the SPAK kinase, we developed a new screening system using ELISA. Previous studies have shown that SPAK possessed very low kinase activity *in vitro*, which hampered a high-throughput screening of the inhibitors.¹⁸ In this study, we adopted a combination strategy that included the recombinant SPAK [T233E] protein, in which the T-loop Thr residue phosphorylated by WNK isoforms was mutated to Glu to mimic phosphorylation, and the Mouse protein 25 α (MO25 α) to detect the SPAK-regulated phosphorylation more sensitively.^{18–20} MO25 α is an enhancer of SPAK kinase. We used a fragment of human NKCC2 (residues 1–174) including SPAK phosphorylation sites as a substrate for SPAK because NKCC2 phosphorylation has been known to be the most detectable during *in vitro* experiments.¹⁸ They were all prepared as glutathione S-transferase (GST) fusion proteins and purified.

First, to determine whether the kinase reaction functions properly *in vitro*, the GST-NKCC2 phosphorylation reaction was confirmed by the immunoblotting of three different anti-phospho-NKCC2 antibodies. As shown in Figure 1, the most dramatic increase in ATP-dependent NKCC2 phosphorylation was observed in the presence of GST-MO25 α . Next, we tested the utility of these anti-phospho-NKCC2 antibodies in the ELISA system. First, the ELISA plates were coated with 5 pmol of GST-NKCC2 [1–174] per well. After this, the kinase reaction was induced on the ELISA plate using GST-SPAK [T233E] with GST-MO25 α in the presence of ATP. Finally, the phosphorylation of GST-NKCC2 was detected with each anti-phospho-NKCC2 antibody. As shown in Figure 2, two of the three anti-phospho-NKCC2 antibodies, pT2 and pNKCC2

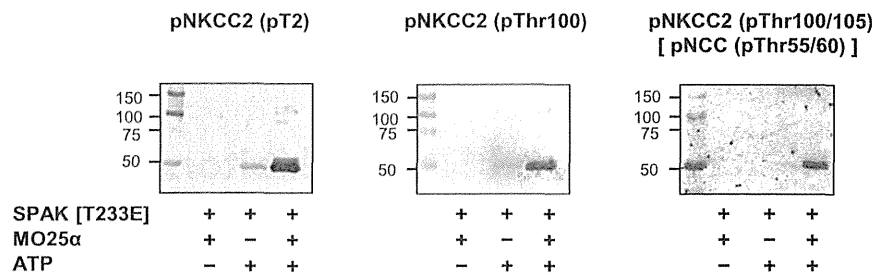


Figure 1. Confirmation of the *in vitro* phosphorylation reaction of GST-NKCC2 using three different anti-phospho-NKCC2 antibodies. GST-NKCC2 is incubated with GST-SPAK [T233E] in the absence or presence of MO25 α . Subsequently, the GST-NKCC2 phosphorylation reaction is confirmed by the immunoblotting by using three different anti-phospho-NKCC2 antibodies: anti-pNKCC2 (pT2), pNKCC2 (pThr100), and pNKCC2 (pThr100/105)[pNCC (pThr50/55)]. The most dramatic increase in ATP-dependent NKCC2 phosphorylation is observed in the presence of GST-MO25 α .

(pThr100/105), succeeded in detecting NKCC2 phosphorylation. Finally, we adopted the anti-phospho-NKCC2 (pThr100/105) antibody as a primary antibody. To determine the dose-dependent kinetics, we incubated 0.5 pmol of GST-SPAK [T233E] in the presence of different concentrations of substrate, GST-NKCC2, and ATP. *In vitro* GST-NKCC2 phosphorylation increased according to the amount of coated GST-NKCC2 (Supplemental Figure 1A) and ATP concentrations (Supplemental Figure 1B). On the basis of these results, we determined that the optimum amounts of GST-NKCC2 and ATP were 5 pmol/well and 0.1 mM, respectively, in this screening.

ELISA Screening of a Small-Molecule Compound Library for SPAK Inhibitors

We applied this newly developed indirect ELISA system for screening approximately 20,000 small-molecule compounds

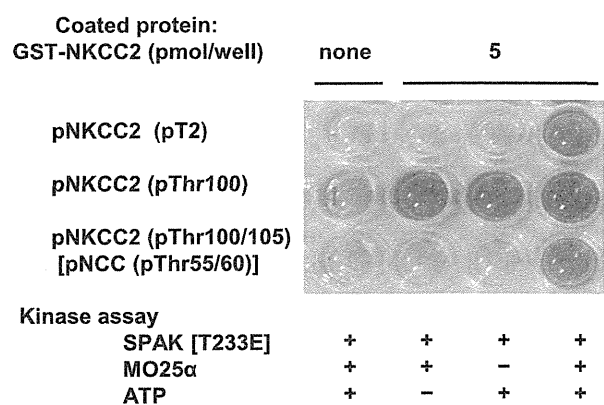


Figure 2. Kinase assay and detection of phosphorylated NKCC2 in the ELISA system. GST-NKCC2 [1–174] is coated to each well of the ELISA plate and incubated with GST-SPAK [T233E] in the presence of GST-MO25 α . Anti-p-NKCC2 (pT2) and p-NKCC2 (pThr100/105) [p-NCC (pTh50/55)] antibodies succeed in detecting NKCC2 phosphorylation. Anti-p-NKCC2 (pThr100) antibody is not appropriate for ELISA, because a nonspecific blue color change also develops in negative control wells.

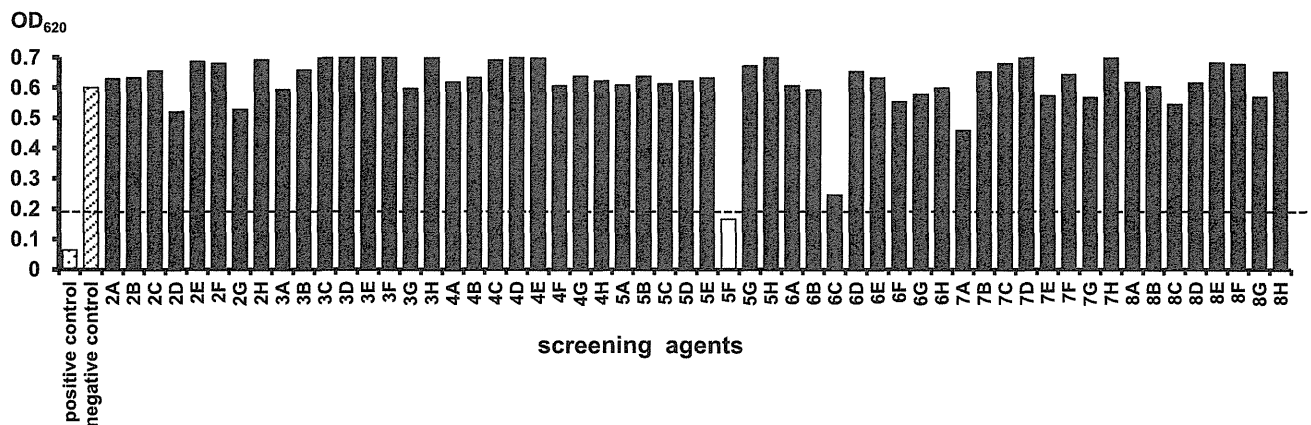


Figure 3. Representative figure of primary screening of SPAK inhibitors in the newly developed ELISA system. Each compound is added in the kinase reaction at a final concentration of 50 μM . As a positive control indicating nonphosphorylation of NKCC2, ATP-free kinase buffer is used. A kinase reaction without any compounds is used as a negative control for screening. The arbitrary cut-off value of OD₆₂₀ is set to 0.2. The compound shown as a white bar is regarded as a positive compound having a strong inhibitory effect on SPAK-regulated NKCC2 phosphorylation.

owned by the Tokyo Medical and Dental University Chemical Biology Screening Center. We actually performed the screening by adding each compound at 50 μM into the kinase reaction buffer and obtained the signals at 620 nm. Representative results of the initial screening are shown in Figure 3. As a result of the initial screening of 21,727 compounds, we found 757 positive compounds. In the secondary assay of these positive compounds, the inhibitory effects were almost the same as those observed in the primary assay (reproducibility was >80%), indicating that our system was solid (Supplemental Figure 2). Subsequently, we carefully narrowed down the candidates by gradually decreasing the final concentrations of the compounds (50–10 μM , data not shown). Finally, we discovered Stock 1S-14279 (1S-14279; PubChem CID 01676700) that showed the highest SPAK inhibitory effect. Figure 4A shows the chemical structure of 1S-14279. The median inhibitory concentration (IC₅₀) value of 1S-14279 for SPAK was 0.26 μM (Figure 4B).

Surface Plasmon Resonance Analyses of the Binding Interactions between 1S-14279 and SPAK Kinase

With our ELISA screening system, it was unclear whether 1S-14279 directly interacts with SPAK. To determine the interaction of 1S-14279 and SPAK, we performed a binding assay using the Biacore system. Gradient concentrations (1.6–12.5 μM) of 1S-14279 were injected

into GST-SPAK-immobilized flow cells. As shown in Figure 4C, 1S-14279 directly bound to SPAK in a concentration-dependent manner. When a simple 1:1 binding model was fitted, the equilibrium constant K_D was 7.0E-6 (M).

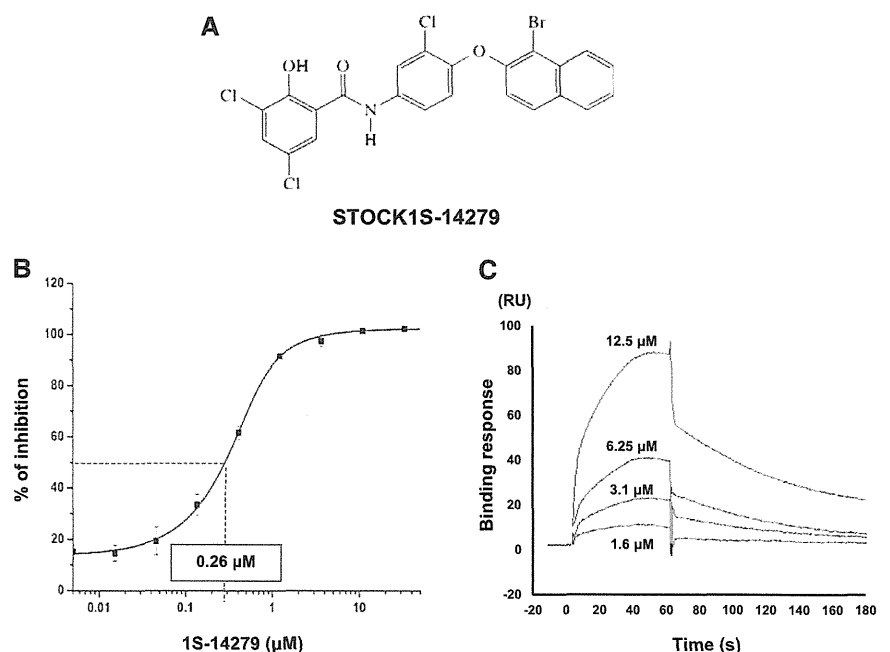


Figure 4. A hit compound obtained from the small-molecule compound library. (A) Chemical structure and substance name of a hit compound. (B) Confirmation of the inhibitory effect of 1S-14279 in the ELISA system. 1S-14279 is added at various concentrations (0.005–50 μM). The IC₅₀ value of 1S-14279 is 0.26 μM ($n=3$, mean \pm SEM). (C) Surface plasmon resonance analysis of 1S-14279 binding to SPAK [T233E]. 1S-14279 is applied at the indicated concentrations. Nonspecific binding to the reference cell is subtracted from each sensorgram to obtain the specific-binding responses. 1S-14279 interacts with SPAK in a concentration-dependent manner. RU, resonance unit.

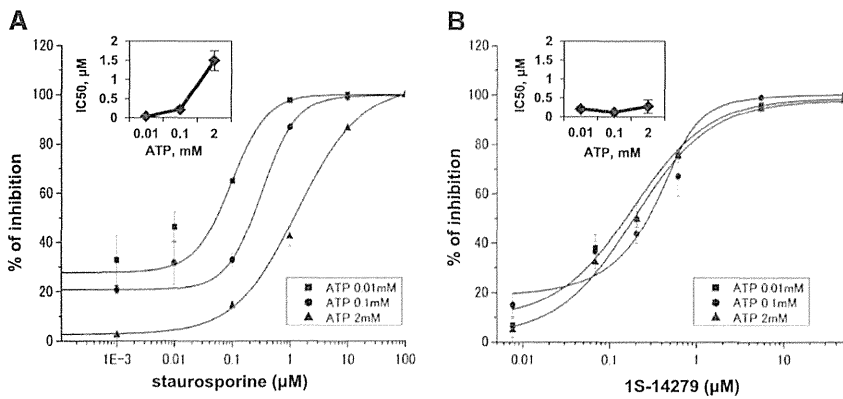


Figure 5. Effect of increasing concentrations of staurosporine and 1S-14279 on SPAK activity at different ATP concentrations in the ELISA system. (A and B) Kinetic data determined for staurosporine (A) and 1S-14279 (B). ATP concentrations in the reaction mixture vary from 0.01 to 2 mM. 1S-14279 and staurosporine are added at various concentrations (from 0.01 to 50 and from 1E-4 to 100 μM , respectively). Data points are the average of three determinations, and the error bars are $\pm\text{SEM}$. The inner panels show IC_{50} values, determined for each ATP concentrations. IC_{50} results are 0.05, 0.27, and 1.6 μM for staurosporine at 0.01, 0.1, and 2 mM ATP, respectively. IC_{50} values of 1S-14279 are not affected by ATP concentration (0.21, 0.13, and 0.26 μM at 0.01, 0.1, and 2 mM ATP, respectively).

Inhibitory Effect of 1S-14279 on SPAK Activity Was Independent of ATP Concentrations

Next, we clarified whether the kinase inhibitory effect of 1S-14279 was due to the competition for ATP bound to SPAK because many kinase inhibitors were ATP competitive. To clarify this issue, we tested the inhibitory effect of 1S-14279 and staurosporine (a nonspecific kinase inhibitor) at different ATP concentrations. Staurosporine interacts with up to 253 human protein kinases with high affinity and inhibits SPAK activity.^{21,22} As shown in Figure 5A, the IC_{50} values of staurosporine as an ATP-competitive inhibitor varied 30-fold (0.05 μM and 1.5 μM at 0.01 mM and 2 mM ATP, respectively). By contrast, the IC_{50} values of 1S-14279 did not alter with the ATP concentration tested (0.21 μM and 0.26 μM at 0.01 mM and 2 mM ATP, respectively) (Figure 5B). These

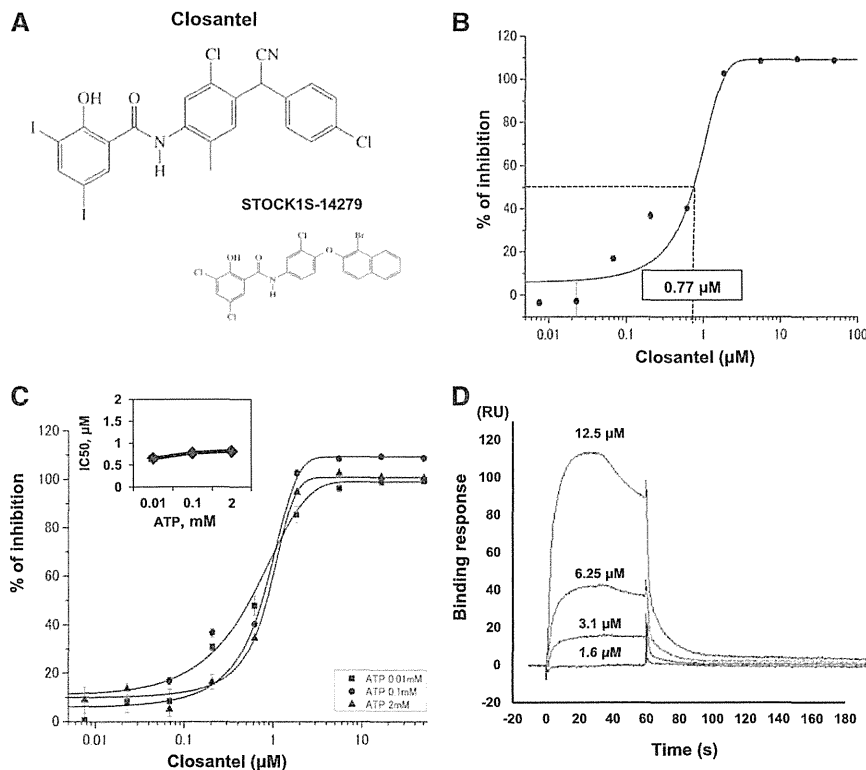


Figure 6. A hit compound obtained from a library of existing drugs. (A) Chemical structure of Closantel and its comparison with 1S-14279. (B) Confirmation of inhibitory effects of Closantel in the ELISA system. The compound is added at various concentrations (0.005–100 μM). The IC_{50} value of Closantel is 0.77 μM ($n=3$, mean \pm SEM). (C) Inhibitory effect of increasing concentrations of Closantel on SPAK activity at different ATP concentrations. Closantel is added at various concentrations (0.01–50 μM). Data points are the average of three determinations, and error bars are $\pm\text{SEM}$. The inner panel shows IC_{50} values determined for each ATP concentrations. IC_{50} values for Closantel are not affected by ATP concentration (0.65, 0.77, and 0.81 μM at 0.01, 0.1, and 2 mM ATP, respectively). (D) Surface plasmon resonance analysis of Closantel binding to SPAK [T233E]. Closantel is applied at the indicated concentrations. Nonspecific binding to the reference cell is subtracted from each sensorgram to obtain the specific-binding responses. Closantel interacts with SPAK in a concentration-dependent manner. RU, resonance unit.

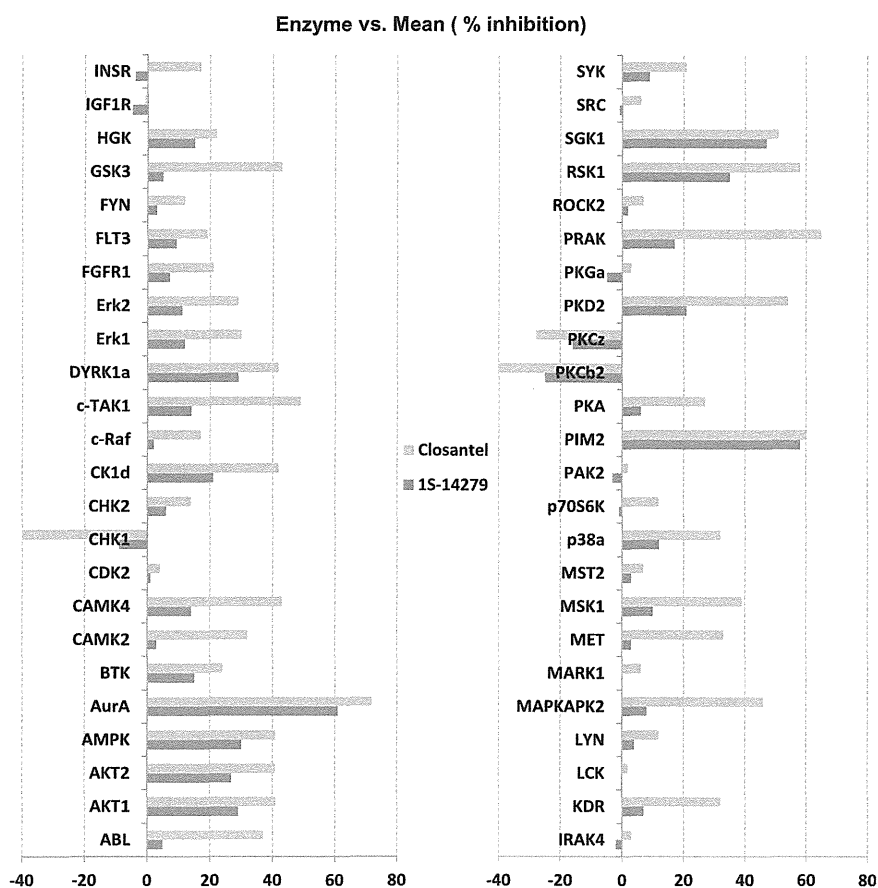


Figure 7. RapidKinaseTM48 panel test of 1S-14279 and Closantel. The percent inhibition of kinase activity is tested at 1.0E-05 M. Mean percent inhibition data are an average of duplicate measurements. AurA, Aurora A kinase; PIM2, Proviral Integrations of Moloney virus 2 kinase.

results clearly suggested that 1S-14279 acts as a non-ATP-competitive inhibitor for SPAK because the inhibitory effect was independent of ATP concentration.²³

Drug Repositioning Strategy to Identify Existing Drugs That Inhibit SPAK Kinase Activity

We further screened a library of 840 existing drugs prepared by our coauthors at Keio University to more efficiently identify clinically applicable SPAK inhibitors. We found that Closantel (*N*-[5-chloro-4-[(4-chlorophenyl)-cyanomethyl]-2-methylphenyl]-2-hydroxy-3,5-di-iodobenzamide), an anthelmintic drug, efficiently inhibited SPAK-regulated NKCC2 phosphorylation *in vitro*. Figure 6A shows the chemical structure of Closantel, which is similar in structure to 1S-14279. Figure 6B shows the results of the concentration-dependent inhibitory effect of Closantel on ELISA. The IC₅₀ value of Closantel was 0.77 μM. Furthermore, we tested the inhibitory effect of Closantel with different ATP concentrations. There was little change in the IC₅₀ values (0.65 μM and 0.81 μM at 0.01 mM and 2 mM ATP, respectively, Figure 6C); this behavior was also similar to that of 1S-14279. In the Biacore systems,

Closantel directly bound to SPAK and showed relatively faster binding and dissociation than 1S-14279.

SPAK Specificity of 1S-14279 and Closantel

To investigate the specificity of these compounds as kinase inhibitors, we conducted a profiling study in the RapidKinase48 panel. The compounds were tested at a final concentration of 1.0E-5 (M), and the kinase profiling revealed that they worked on a few serine/threonine kinases such as Aurora A kinase and Proviral Integration of Moloney virus 2 kinase, although the inhibition did not exceed 80% (Figure 7). Although SPAK kinase was not included in this panel, our ELISA assay showed an IC₅₀ of Closantel and 1S-14279 for SPAK in the range of 1.0E-7 (M), suggesting that both compounds have a potential to behave as specific SPAK inhibitors at lower concentrations.

1S-14279 and Closantel Showed Inhibitory Effects on Hypotonicity-Induced WNK-SPAK-NCC/NKCC Signaling in Mouse Renal Distal Tubule-Derived Cells and Vascular Smooth Muscle Cells

To test whether these compounds possess an *in vivo* inhibitory effect against SPAK, we used mouse renal distal tubule-derived (mpkDCT) cells and mouse vascular smooth muscle (MOVAS) cells, which endogenously express NCC and NKCC1, and performed cell-based inhibitory assays.^{6,24} We used 30-minute hypotonic shock (170 mOsm/g H₂O) to activate WNK-SPAK-NCC/NKCC signaling.²⁵ Both 1S-14279 and Closantel demonstrated a dose-dependent inhibitory effect of phosphorylation of endogenous NCC (pThr53) in mpkDCT cells (Figures 8A and 9A) and of NKCC1 (pThr206) in MOVAS cells (Figures 8B and 9B). To exclude the possibility that the decrease in phosphorylation was due to nonspecific effects, we evaluated the effect of these compounds on phospho-p38 MAPK expression, which is an isolated phosphorylation event from WNK-SPAK signaling.²⁶ As shown in Figures 8 and 9, even with the high concentration of these compounds, the phosphorylation of p38 expression was not reduced but was slightly increased. These data support the specificity of the inhibitory effect of 1S-14279 and Closantel on SPAK activity.

Acute Effects of 1S-14279 and Closantel in Mice

To define whether these compounds are effective in animals, we examined NCC and NKCC2 phosphorylation in the kidney and NKCC1 phosphorylation in the aorta of mice intraperitoneally

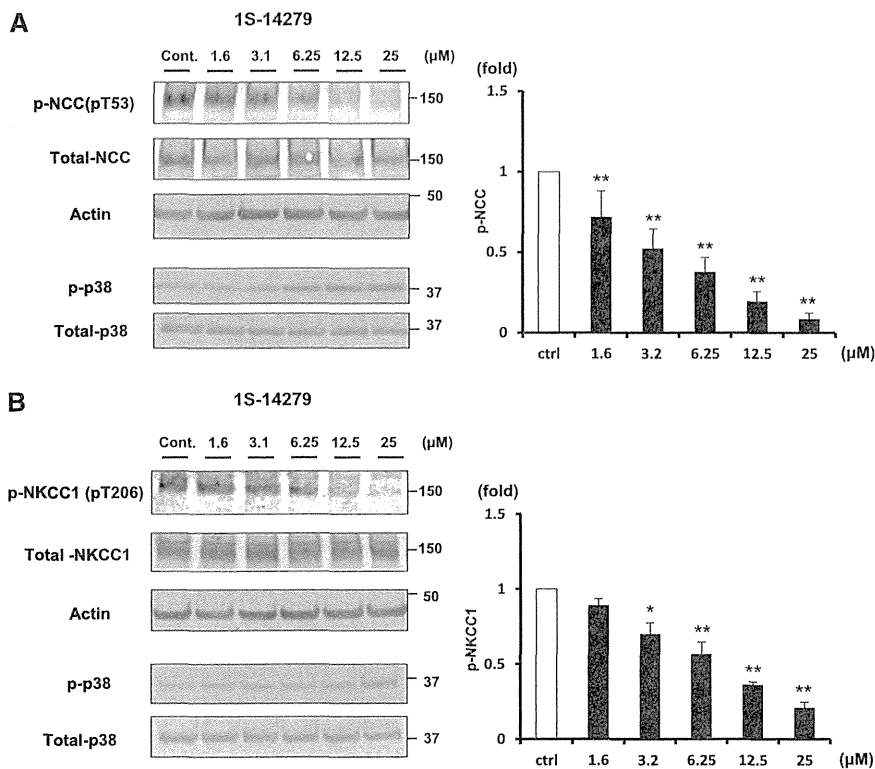


Figure 8. Inhibitory effect of 1S-14279 on WNK-SPAK-NCC/NKCC1 signaling in mpkDCT and MOVAS cells. (A) The left panel shows the inhibitory effect of 1S-14279 in mpkDCT cells. The phosphorylation of NCC in mpkDCT cells is drastically and dose-dependently reduced by 1S-14279 (1.6–25 μM). The right panel shows quantification of the results of the blots ($n=4$, mean±SEM). (B) The left panel shows the inhibitory effect of 1S-14279 in MOVAS cells. The phosphorylation of NKCC1 is drastically and dose-dependently reduced by 1S-14279 (1.6–25 μM). The right panel shows quantification of the results of the blots ($n=4$, mean±SEM). * $P<0.05$; ** $P<0.01$. Cont/ctrl, control.

injected with 20 mg/kg of 1S-14279 or Closantel. As shown in Figures 10A and 11A, markedly reduced NCC phosphorylation (pSer71) with total NCC reduction was observed in the kidneys after 30 minutes of drug administration. On the other hand, NKCC2 phosphorylation (pThr96), which was mainly regulated by OSR1 but not SPAK,²⁷ was not affected. To exclude the non-specific effects of the compounds, we also evaluated the effect of these compounds on phospho-p38 MAPK expression, as mentioned in the cell-based inhibitory assay. Even with the administration of these compounds, the expression of phospho-p38 was not reduced and was slightly increased, similar to that observed in the cell-based study. Similarly, NKCC1 phosphorylation (pThr206) at the SPAK phosphorylation site was reduced in the aorta. We also followed the time course of the inhibitory effect after a single injection of 1S-14279 and Closantel. After 30 minutes of injection, the level of phosphorylated NCC rapidly decreased; however, it entirely recovered after 120 minutes (Supplemental Figure 3). The SPAK inhibitory effects of 1S-14279 and Closantel were short acting and reversible. We then chose Closantel for BP measurement because preliminary experiments revealed that mice typically died after repeated injection of

1S-14279, and Closantel showed no lethal effects. As shown in Figure 12, the acute injection of Closantel induced marked hypotension from baseline, which was greatest immediately after injection. The heart rate also decreased just after the hypotensive reaction and recovered earlier than the BP.

Effect of Chronic Closantel Treatment in Mice

Next, we examined the effect of chronic treatment with oral Closantel. C57BL/6 mice were fed the mouse chow containing Closantel at a dosage of 300 mg/kg per day. Mice appeared to be healthy during the Closantel treatment. As shown in Figure 13, by day 7 of treatment, NCC and NKCC2 phosphorylation were markedly decreased in the kidneys, and NKCC1 phosphorylation was reduced in the aorta. However, BP was not decreased by Closantel, and we observed no significant differences in serum and urine electrolytes between the Closantel and control groups (Supplemental Figure 4, Supplemental Table 1).

DISCUSSION

We previously reported that the constitutive activation of the WNK-OSR1/SPAK-NCC signal cascade is the major pathogenic mechanism of PHAII.^{28–30} The increased level of NCC phosphorylation induces excessive NaCl reabsorption and causes salt-sensitive hypertension. WNK-OSR1/SPAK kinase also phosphorylates and activates NKCC1 in vascular smooth muscle cells and leads to vasoconstriction.^{7–10} Furthermore, we revealed that this cascade was activated not only in PHAII but also in hyperinsulinemic conditions and could also cause salt-sensitive hypertension.¹³ Therefore, drugs that inhibit this signal cascade could become new antihypertensive drugs that have dual effects as a diuretic and vasodilator and could be particularly beneficial for patients with hyperinsulinemia (e.g., metabolic syndrome and obesity). However, directly inhibiting WNK kinases could have a risk of unexpected adverse reactions because homozygous WNK1 and OSR1 knockout mice are embryonically lethal. On the other hand, it was previously reported that SPAK knockout mice were not fatal and displayed hypotension with low NCC and NKCC1 phosphorylation in the kidney and aorta, respectively.^{16,17} Thus, the SPAK kinase may become a prime target for drug development with the inhibition this signal cascade.

In this study, we sought to develop a new screening system using ELISA that could demonstrate SPAK-regulated phosphorylation *in vitro*. As a result of our screening, we discovered

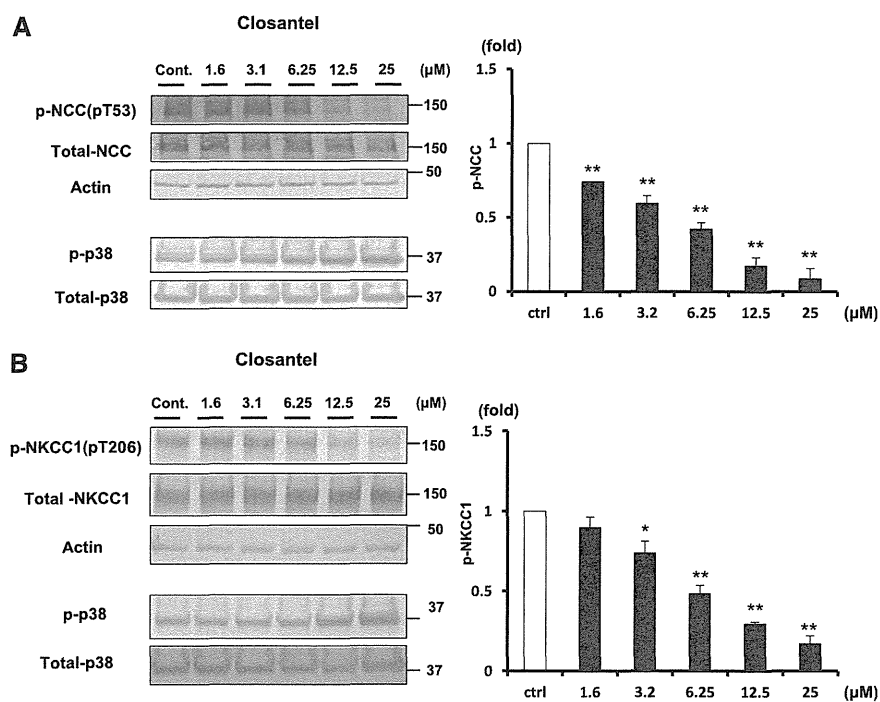


Figure 9. Inhibitory effect of Closantel on WNK-SPAK-NCC/NKCC1 signaling in mpkDCT and MOVAS cells. (A) The left panel shows the inhibitory effect of Closantel in mpkDCT cells. The phosphorylation of NCC in mpkDCT cells is drastically and dose-dependently reduced by Closantel (1.6–25 μ M). The right panel shows quantification of the results of the blots ($n=4$, mean \pm SEM). (B) The left panel shows the inhibitory effect of Closantel in MOVAS cells. The phosphorylation of NKCC1 is drastically and dose-dependently reduced by Closantel (1.6–25 μ M). The right panel shows quantification of the results of the blots ($n=4$, mean \pm SEM). * $P<0.05$; ** $P<0.01$. Cont/ctrl, control.

two hit compounds: 1S-14279 from a small-molecule compound library and Closantel from a library of existing drugs. Surprisingly, these two compounds had quite similar constitutions and both possessed strong SPAK inhibitory effects not only *in vitro* but also in cultured cell lines and in mice. Closantel is widely used as an antiparasitic agent in livestock either parenterally or orally at a single dose of 5–10 mg/kg. Some observations in humans for the treatment of liver fluke disease have been reported (E. Bernardiner, unpublished data). In recent years, the so-called drug repositioning strategy, in which an existing drug currently used for a specific disease is applied to another disease, has gained increasing attention from both academia and industry.³¹ An advantage of this strategy is that existing drugs have already passed several stages of clinical development, which could reduce the development risk and costs. In this study, we identified a novel function of Closantel, which appeared to be less toxic than 1S-14279 because mice tolerated chronic treatment with Closantel, but not with 1S-14279. Closantel is a salicylanilide derivative that acts as an uncoupler of the oxidative phosphorylation in the cell mitochondria, which disturbs ATP production. However, in our study, another salicylanilide, oxyclozanide, had no SPAK inhibitory effect (data not shown). The compound

structure of Closantel was quite important in the exertion of inhibitory actions on SPAK and the constitutional similarity of 1S-14279; Closantel may give us clues to the synthesis of compounds that have higher efficacy and less toxicity through further structural three-dimensional analysis.

It is noteworthy that both Closantel and 1S-14279 acted as non-ATP-competitive SPAK inhibitors. Most protein kinase inhibitors show an ATP-competitive type of kinase inhibition, which makes it difficult to determine high specificity because the human kinome is composed of >500 protein kinases that share a high degree of identity in the ATP binding pocket. Moreover, ATP-competitive inhibitors must compete with high intracellular ATP levels, leading to a discrepancy between IC_{50} values measured during an *in vitro* study versus those measured during an *in vivo* study.³² Thus, the ATP intensiveness of Closantel and 1S-14279 would be a clear advantage in generating highly specific inhibitors for SPAK.

In this study, we demonstrated that acute and chronic Closantel administration successfully decreased the expression of both phospho-NCC in the kidney and phospho-NKCC1 in the aorta. Similar results were observed in our previous studies with SPAK knockout mice.¹⁷ After acute Closantel administration, the BP decreased very rapidly, suggesting that at least in the acute phase, the vasorelaxing effect of SPAK inhibition might be dominant over its natriuretic effect. Although heart rate also decreased, whether this resulted from specific SPAK inhibition and contributed to the decrease in BP requires further investigation. The involvement of SPAK in regulating intracellular Na^+ and Cl^+ in cardiomyocytes has been reported,^{33,34} and an unidentified role of SPAK in the heart could be clarified by the discovery of SPAK inhibitors. Unfortunately, the natriuretic action of acute Closantel treatment could not be confirmed because we could not reproducibly collect urine samples in the short experimental period (the duration of activity of Closantel was too short to exert a diuretic effect; Supplemental Figure 3). In addition, we observed no significant increases in sodium excretion under chronic Closantel administration, although this may not be surprising given that SPAK knockout mice showed no such increase.¹⁷ Experiments using larger animals and ureteric cannulation are necessary for detailed analysis of Closantel on kidney functions. Furthermore, hypertensive models are needed to assess the antihypertensive effect of Closantel, which may not have an effect on baseline BP like other antihypertensive drugs. Nevertheless, this study could clearly demonstrate that chronic Closantel treatment could inhibit SPAK.

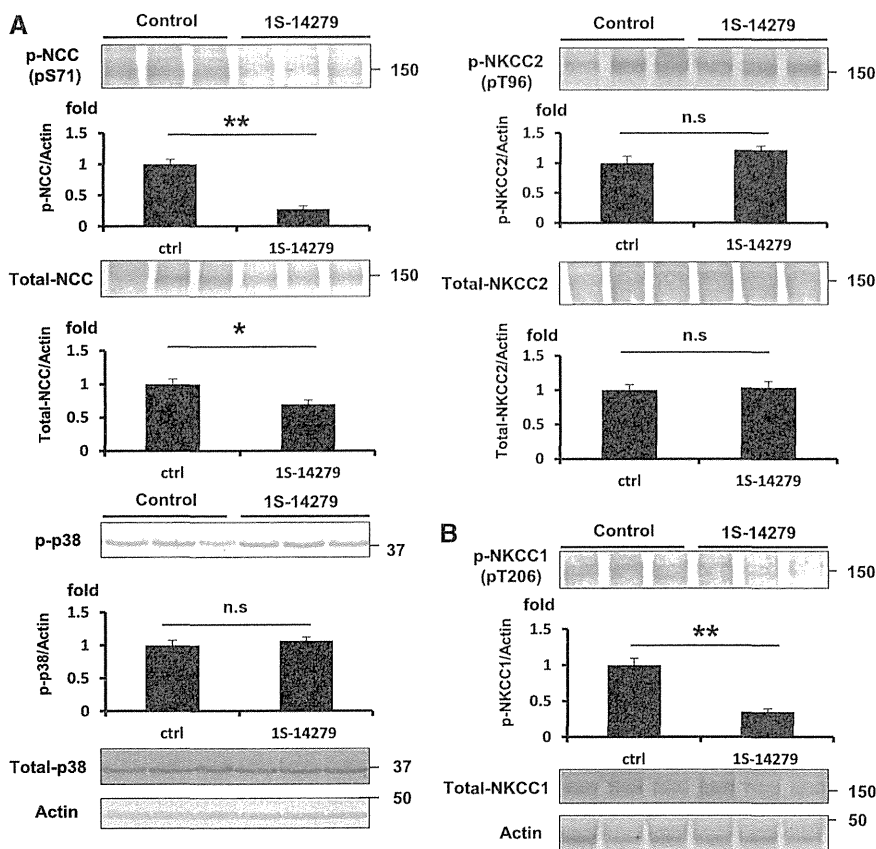


Figure 10. Inhibitory effect of 1S-14279 on WNK-SPAK-NCC/NKCC1 signaling in mouse kidney and aorta. (A) Representative immunoblots of total- and p-NCC, NKCC2, and p38 of the kidney at 30 minutes after infusion of 1S-14279. The NCC phosphorylation is drastically reduced by 1S-14279. No significant increases in pNKCC2 and p-p38 levels are observed. The lower panel shows quantification of the results of the blots ($n=4$, mean \pm SEM). (B) Representative immunoblots of total- and p-NKCC1 of the aorta at 30 minutes after infusion of 1S-14279. The expression of p-NKCC1 is markedly reduced. No significant difference in total NKCC1 abundance. The lower panel shows quantification of the results of the blots ($n=4$, mean \pm SEM). * $P<0.05$; ** $P<0.01$. Ctrl, control.

Furthermore, OSR1 could also be inhibited by chronic Closantel treatment based on the observation that NKCC2 phosphorylation, which is mainly regulated by OSR1,¹⁷ was decreased. This is plausible given that SPAK and OSR1 share high homology in their catalytic and regulatory domains.¹⁷

In conclusion, we found two hit compounds that inhibit SPAK kinase both *in vitro* and *in vivo*. Further pharmacologic modification of these compounds and their *in vivo* validation in other animal species and disease models could lead to the development of a novel antihypertensive drug.

CONCISE METHODS

Molecular Cloning and Plasmid Construction

The pRK5 expression plasmid containing T7-tagged whole SPAK was kindly provided by T. Moriguchi and H. Shibuya (Tokyo Medical and Dental University). The active SPAK [T233E] mutation¹⁸ was

introduced using the QuickChange Site-Directed Mutagenesis Kit (Agilent Technologies Inc., Santa Clara, CA) and cloned into the pGEX6p bacterial expression vector (GE Healthcare UK Ltd.). To clone human NKCC2 [1–174], RT-PCR was carried out using human kidney mRNA as a template, and the resulting PCR product was cloned into the pGEX6p bacterial expression vector. MO25 α cDNA was generated by RT-PCR using mouse kidney mRNA as a template, and cloned into the pGEX6p expression vector.

Expression of GST-Tagged Fusion Proteins in *Escherichia coli*

All recombinant GST fusion proteins were transformed into BL21 *E. coli* cells. One-liter cultures of the transformed *E. coli* were grown at 37°C in 2-YT broth containing 100 μ g/ml ampicillin until the absorbance value at 600 nm reached 0.5. Isopropyl-D-galactosidase (0.2 mM) was then added to induce protein expression, and the cells were cultured for an additional 16 hours at 28°C. The cells were then collected by centrifugation at 4°C, lysed by sonication in 40 ml of ice-cold 1 \times PBS buffer containing Complete Protease Inhibitors (Roche Diagnostics), and incubated with 1% Triton X-100 and 0.5% salcosyl. The GST-tagged proteins were purified from the lysates using 1.2 ml of glutathione-Sepharose beads and eluted in an elution buffer containing 83 mM Tris-HCl, 150 mM KOH, and 30 mM glutathione.²⁶

Antibodies and Immunoblotting Analyses

Quantitative immunoblotting was performed as previously described.⁴ Blots were probed with the following primary antibodies: anti-total

NCC,³⁵ anti-phosphorylated NCC (pThr53 and pSer71 in mouse NCC),¹¹ anti-total NKCC1 (T4) (Hybridoma Bank, University of Iowa, Iowa City, IA), anti-phosphorylated NKCC1 (pThr206 in mouse NKCC1),²⁷ anti-total NKCC2 (Alpha Diagnostic, San Antonio, TX), anti-phosphorylated NKCC2 (pThr100 in human NKCC2),³⁶ anti-phosphorylated NKCC2 (termed pT2 antibody; kindly provided by K. Mutig),³⁷ anti-phosphorylated p38, anti-total p38 (Cell Signaling Technology, Danvers, MA), and anti-actin (Cytoskeleton, Denver, CO). Rabbit antiserum against phosphorylated NCC [residues 49–64 of mouse NCC phosphorylated at Thr53/58; Cys+LYMR(pT)FGYN (pT)IDVVPV] was generated and affinity purified. This antibody could be used to detect the phosphorylation of human NKCC2 at residues Thr100/105, which are equivalent to Thr55/60 in human NCC and Thr53/58 in mouse NCC. Alkaline phosphatase-conjugated anti-IgG antibodies (Promega, Madison, WI) were used as secondary antibodies and Western Blue (Promega) was used as a substrate for signal detection. The intensity of the bands was analyzed and quantified using ImageJ software (National Institutes of Health, Bethesda, MD).

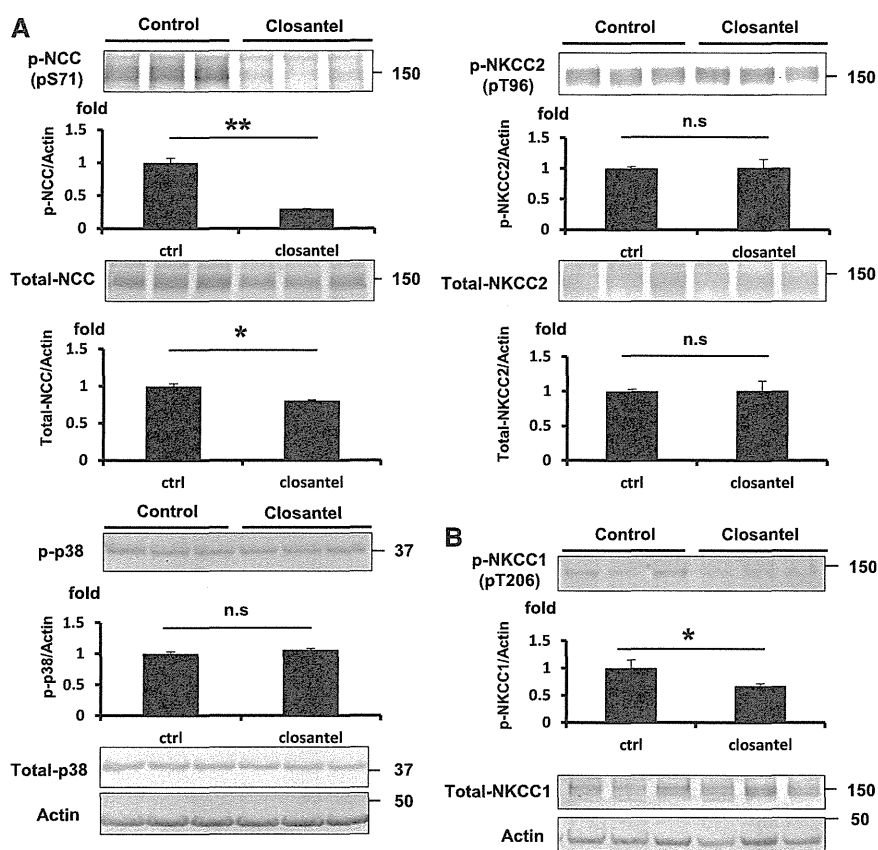


Figure 11. Inhibitory effect of Closantel on WNK-SPAK-NCC/NKCC1 signaling in mouse kidney and aorta. (A) Representative immunoblots of total- and p-NCC, NKCC2 and p38 of the kidney at 30 minutes after infusion of Closantel. The NCC phosphorylation is drastically reduced by Closantel. No significant increases in pNKCC2 and p-p38 levels are observed. The lower panel shows quantification of the results of the blots ($n=3$, mean \pm SEM). (B) Representative immunoblots of total- and p-NKCC1 of the aorta at 30 minutes after infusion of Closantel. The expression of p-NKCC1 is markedly reduced. No significant difference in total NKCC1 abundance. The lower panel shows quantification of the results of the blots ($n=4$, mean \pm SEM). * $P<0.05$; ** $P<0.01$. Ctrl, control.

In Vitro Kinase Assays

GST-NKCC1 [1–174] protein (7 μ g) purified from *E. coli* was incubated with 1 μ g of GST-SPAK [T233E] and 5 μ g of GST-MO25 α . Kinase assay reactions were performed for 60 minutes at 30°C in a 25 μ l of kinase reaction buffer (50 mM Tris-HCl [pH 7.5], 1 mM dithiothreitol, 1 mM EGTA) containing 10 mM MgCl₂ and 0.1 mM ATP as previously described.⁶ The reactions were stopped by the addition of SDS sample buffer (Cosmo Bio Inc., Tokyo, Japan) followed by denaturation for 20 minutes at 60°C. The reaction products were analyzed by SDS-PAGE.

Chemical Screening Using an Indirect ELISA System

GST-NKCC2 [1–174] (5 pmol/well) in a bicarbonate buffer (15 mM Na₂CO₃, 35 mM NaHCO₃) was applied to 96-well ELISA plates (Iwaki & Co., Ltd., Tokyo, Japan) and incubated overnight at 4°C for immobilization. After blocking with 1.5% (w/v) albumin in tris-buffered saline (TBS)-0.02% Tween 20 for 30 minutes at room temperature, kinase reactions were performed in 100 μ l of kinase reaction buffer containing

10 mM MgCl₂, 0.1 mM ATP, 0.5 pmol of GST-SPAK [T233E], and 5 pmol of GST-MO25 α . After a 1-hour incubation at 30°C under gentle shaking, the plates were washed five times with wash buffer (TBS-0.02% Tween 20) using a Microplate Washer (ImmunoWash 1575; Bio-Rad, Mississauga, ON, Canada). Subsequently, 100 μ l of 1.5 μ g/ml rabbit anti-pNKCC2 antibody (pThr100/105; NCC pThr55/60) was applied to each well for the pNKCC2 assay and incubated overnight at 4°C. After washing, 100 μ l of alkaline phosphatase-labeled anti-rabbit secondary antibody was added to each well and the plates were incubated for 1 hour at 37°C. After washing, 100 μ l of BluePhos (KPL Inc., Gaithersburg, MD) was applied to each well, and the blue color developed was measured by reading the absorbance at 620 nm in a microplate reader (Spectrafluor; Tecan Japan Co., Ltd., Kanagawa, Japan). For chemical library screening, each compound was added to the kinase reaction at a final concentration of 50 μ M. For inhibition studies, increasing concentrations of each compound were tested in triplicate. Curve fitting was performed using ORIGIN8.1 data analysis and graphing software (OriginLab Co., Ltd., Northampton, MA), and data are presented as the mean \pm SEM. Stock solutions of compounds, in 100% DMSO, were diluted with water to a final DMSO concentration of 1%. Controls without inhibitors were also incubated in the presence of 1% DMSO.

Kinetic Binding Analyses Using a Biacore Biosensor

The binding kinetics between SPAK and the various compounds were analyzed using a

Biacore T100 system (GE Healthcare UK Ltd.). CM5 sensor chips were docked and GST-SPAK [T233E] was injected for 7 minutes at a flow rate of 10 μ l/min over the surface after preactivation with a mixture of 0.2 M 1-ethyl-3-[3-dimethylaminopropyl]carbodiimide hydrochloride and 0.05 M sulfo-*N*-hydroxysuccinimide. After the injection of GST-SPAK [T233E], the surface was deactivated with 150 μ l of 1 M ethanolamine HCl (pH 8.5), giving an immobilization level for GST-SPAK [T233E] of approximately 10,000 resonance units. To reduce nonspecific binding, we used a reference surface immobilized with GST at 3000 resonance units. The TBS-based buffer (50 mM Tris-HCl [pH 7.5], 150 mM NaCl, 10 mM MgCl₂, 0.05% surfactant-P) with 5% DMSO was used as a running buffer to facilitate dissolution of the compounds, and the temperature was set to 25°C. Analysis of the interactions between the small-molecule compounds and GST-SPAK [T233E] was carried out using a one-shot kinetic approach. For each compound, a series of solutions of four different concentrations and a blank sample for double referencing were injected for 60 seconds at a flow rate of 90 μ l/min. No regeneration was applied. The sensorgrams

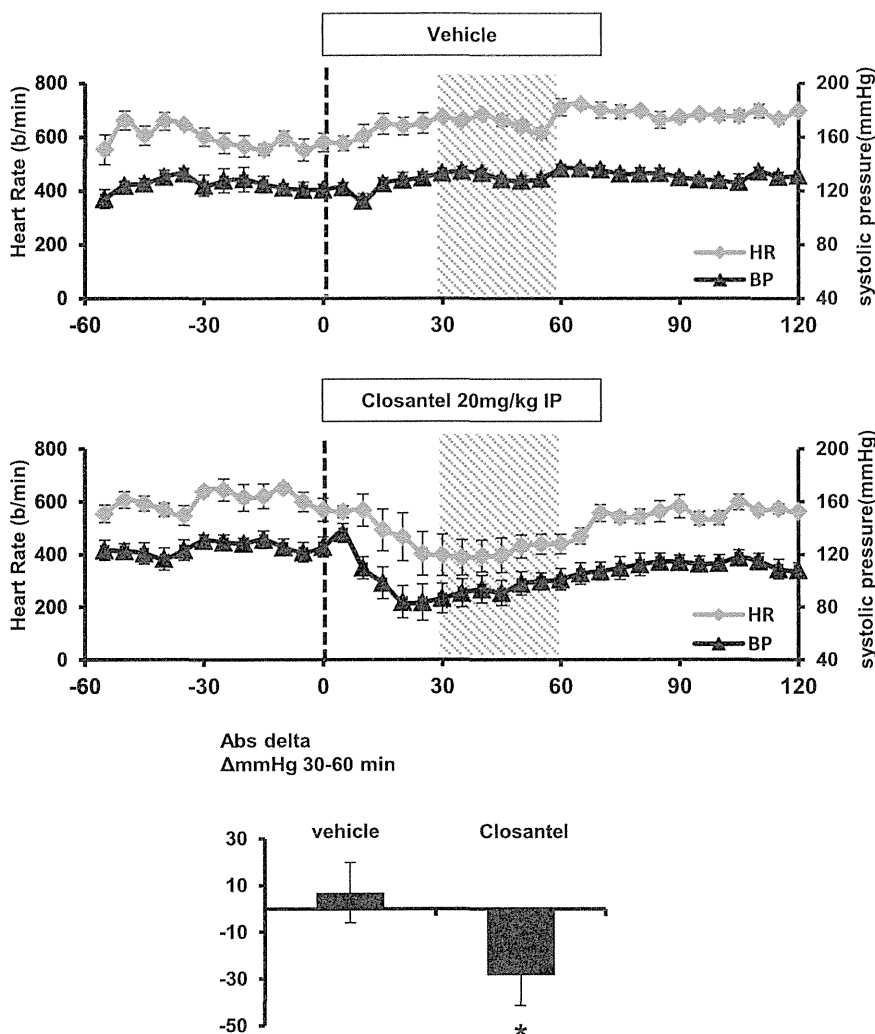


Figure 12. Acute Closantel administration-induced hypotension in mice. The line graphs represent the systolic arterial BP (black triangles; $n=5$) and heart rate (gray diamonds; $n=5$) before and after vehicle (40% DMSO) and Closantel (20 mg/kg in 40% DMSO) administration. The dashed vertical lines indicate the beginning of drug administration. The shaded area represents the period under analysis. The bar graphs show the average decrease in systolic arterial pressure during the 30- to 60-minute postinjection period ($*P<0.05$; $n=5$, mean \pm SEM). Closantel induces a marked reduction in the BP, which appears to precede the decrease in the heart rate, and persists longer. HR, heart rate; IP, intraperitoneal; Ab, antibody.

were processed and fitted to determine the dissociation constants using Biacore T100 evaluation software.

Kinase Profiling

Kinase profiling was conducted by PerkinElmer (Boston, MA) using a RapidKinase48 panel in duplicate wells. The compounds were tested at a final concentration of $1.0E-5$ (M). Each test compound was incubated with each of the kinases and appropriate substrates according to PerkinElmer standard operating procedures. After the incubation period, the reaction products and remaining substrate were measured. According to PerkinElmer guidelines, compounds that show $\geq 50\%$ inhibition are considered active.

Cell Culture and Inhibition Assay

The mpkDCT cell line kindly provided by A. Vandewalle was cultured in a defined medium as previously described.³⁸ MOVAS cells were cultured in DMEM supplemented with 10% (v/v) FBS, 2 mM L-glutamine, 100 U/ml penicillin, and 0.1 mg/ml streptomycin at 37°C in a humidified 5% CO₂ incubator. mpkDCT and MOVAS cells were cultured on six-well dishes. Hypotonic stimulation was performed as previously reported.²⁶ For the inhibition assay, cells were exposed to each compound for 30 minutes and then stimulated with a hypotonic low-chloride medium for 30 minutes.²⁵ Cells were then lysed in 0.15 ml of ice-cold cell lysis buffer (50 mM Tris-HCl [pH 7.5], 150 mM NaCl, 1 mM EGTA, 1 mM EDTA, 50 mM sodium fluoride, 1 mM sodium orthovanadate, 1% Triton X-100, 0.27 M sucrose, 1 mM dithiothreitol) per well. After centrifugation at $12,000\times g$ for 5 minutes at 4°C, the supernatants were denatured for 20 minutes at 60°C with SDS sample buffer and subjected to SDS-PAGE.

Animal Studies

Female C57BL/6 mice (10 weeks old) were obtained and received standard laboratory chow and water. The Animal Care and Use Committee of Tokyo Medical and Dental University approved the experimental protocol. In an acute treatment study, 1S-14279 and Closantel were both administered intraperitoneally at a dose of 20 mg/kg in 40 μ l of DMSO; the control mice were administered 40 μ l of DMSO alone. The mice were euthanized 30 minutes after injection. In the chronic treatment study, C57BL/6 mice were fed the mouse chow containing Closantel at a dosage of 300 mg/kg per day. The kidney was removed and rapidly homogenized in a 10-fold mass excess of ice-cold 1% (w/v) Triton X-100 lysis buffer. Whole homogenates without the nuclear fraction ($600\times g$) were collected and denatured at 60°C for 20 minutes as previously reported.⁴ The aorta was

rapidly isolated and frozen with liquid nitrogen. After being crushed by sonication, aortas were added to 150 μ l of lysis buffer as previously reported,⁷ and centrifuged at $6000\times g$ for 5 minutes at 4°C. A 120- μ l aliquot of the supernatant was denatured at 60°C for 20 minutes. The total protein concentration was determined by the Bradford method using BSA as a standard, and lysates were stored at -80°C. Quantitative immunoblotting was performed as previously described.¹² The relative intensities of immunoblot bands were determined by densitometry using ImageJ software.

The BP of the mice was measured using a radiotelemetric method in which a BP transducer (Data Sciences International, St. Paul, MN) was inserted into the left carotid artery. The mice were housed individually

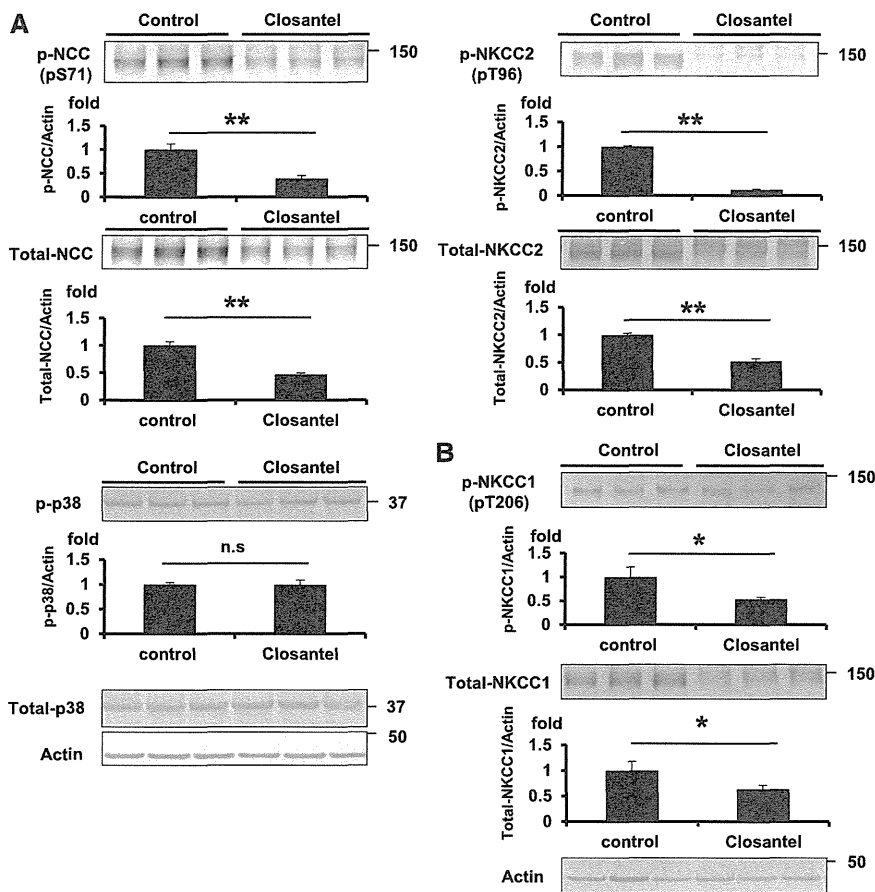


Figure 13. Inhibitory effect of chronic Closantel treatment on WNK-SPAK-NCC/NKCC1 signaling in mouse kidney and aorta. The dosage of Closantel added to the mouse chow is 300 mg/kg per day. (A) Representative immunoblots of total- and p-NCC and NKCC2 after 7 days treatment of Closantel. NCC and NKCC2 phosphorylation are markedly reduced by Closantel. The lower panel shows the quantification of the results of the blots ($n=4$, mean \pm SEM). (B) Representative immunoblots for the total- and p-NKCC1 of the aorta after 7 days Closantel administration. The expression of p-NKCC1 is markedly reduced. The lower panel shows the quantification of the results of the blots ($n=4$, mean \pm SEM). * $P < 0.05$; ** $P < 0.01$.

in a standard cage with a 12-hour/12-hour light/dark cycle and received standard laboratory chow and water as previously described.³⁹ Seven days after transplantation, the systolic and diastolic arterial pressures were recorded 1 hour before and 2 hours after intraperitoneal injections of either 20 mg/kg Closantel dissolved in 40% DMSO or 40% DMSO alone as a vehicle control. All drugs were freshly prepared in DMSO each day, and the effect of each drug or vehicle was assessed on separate days. Blood was drawn from the retro-orbital sinus under light ether anesthesia. Serum data were determined using the i-STAT system (FUSO Pharmaceutical Industries, Osaka, Japan). Urine electrolytes were determined using a Fuji DRI-CHEM 4000 system (FujiFilm, Tokyo, Japan). Serum and urine creatinine concentrations were determined using a commercial kit (LabAssay Creatinine; Wako Chemical Inc., Osaka, Japan).

Statistical Analyses

Data are expressed as the mean \pm SEM. Comparisons between the two groups were performed with unpaired t tests. P values < 0.05 were considered statistically significant.

ACKNOWLEDGMENTS

We thank Makiko Nawa (Laboratory of Cytometry and Proteome Research, Tokyo Medical and Dental University) for her help with Biacore analysis. We also thank Dr. K. Mutig and A. Vandewalle for the provision of pT2 antibody and mpkDCT cells, respectively.

This study was supported in part by Grants-in-Aid for Scientific Research (S) and (A) from the Japan Society for the Promotion of Science; a Grant-in-Aid for Young Scientists (B) from the Ministry of Education, Culture, Sports, Science and Technology of Japan; a Health and Labor Sciences Research Grant from the Ministry of Health, Labor and Welfare of Japan; and grants from the Salt Science Research Foundation (no. 1422), the Takeda Science Foundation, the Banyu Foundation, and the Vehicle Racing Commemorative Foundation.

DISCLOSURES

None.

REFERENCES

- Shimkets RA, Warnock DG, Bositis CM, Nelson-Williams C, Hansson JH, Schambelan M, Gill JR Jr, Ulick S, Milora RV, Findling JW, Canessa CM, Rossier BC, Lifton RP: Liddle's syndrome: Heritable human hypertension caused by mutations in the beta subunit of the epithelial sodium channel. *Cell* 79: 407–414, 1994
- Achard JM, Disse-Nicodeme S, Fiquet-Kempf B, Jeunemaitre X: Phenotypic and genetic heterogeneity of familial hyperkalaemic hypertension (Gordon syndrome). *Clin Exp Pharmacol Physiol* 28: 1048–1052, 2001
- Wilson FH, Disse-Nicodeme S, Choate KA, Ishikawa K, Nelson-Williams C, Desitter I, Gunel M, Milford DV, Lipkin GW, Achard JM, Feely MP, Dussol B, Berland Y, Unwin RJ, Mayan H, Simon DB, Farfel Z, Jeunemaitre X, Lifton RP: Human hypertension caused by mutations in WNK kinases. *Science* 293: 1107–1112, 2001
- Yang SS, Morimoto T, Rai T, Chiga M, Sohara E, Ohno M, Uchida K, Lin SH, Moriguchi T, Shibuya H, Kondo Y, Sasaki S, Uchida S: Molecular pathogenesis of pseudohypoaldosteronism type II: Generation and analysis of a Wnk4(D561A/+) knockin mouse model. *Cell Metab* 5: 331–344, 2007
- Wakabayashi M, Mori T, Isobe K, Sohara E, Susa K, Araki Y, Chiga M, Kikuchi E, Nomura N, Mori Y, Matsuo H, Murata T, Nomura S, Asano T, Kawaguchi H, Nonoyama S, Rai T, Sasaki S, Uchida S: Impaired KLHL3-mediated ubiquitination of WNK4 causes human hypertension. *Cell Reports* 3: 858–868, 2013
- Richardson C, Rafiqi FH, Karlsson HK, Moleleki N, Vandewalle A, Campbell DG, Morrice NA, Alessi DR: Activation of the thiazide-sensitive Na⁺-Cl⁻ cotransporter by the WNK-regulated kinases SPAK and OSR1. *J Cell Sci* 121: 675–684, 2008
- Zeniya M, Sohara E, Kita S, Iwamoto T, Susa K, Mori T, Oi K, Chiga M, Takahashi D, Yang SS, Lin SH, Rai T, Sasaki S, Uchida S: Dietary salt

- intake regulates WNK3-SPAK-NKCC1 phosphorylation cascade in mouse aorta through angiotensin II. *Hypertension* 62: 872–878, 2013
8. Meyer JW, Flagella M, Sutliff RL, Lorenz JN, Nieman ML, Weber CS, Paul RJ, Shull GE: Decreased blood pressure and vascular smooth muscle tone in mice lacking basolateral Na(+)-K(+)-2Cl(-) cotransporter. *Am J Physiol Heart Circ Physiol* 283: H1846–H1855, 2002
 9. Akar F, Jiang G, Paul RJ, O'Neill WC: Contractile regulation of the Na (+)-K(+)-2Cl(-) cotransporter in vascular smooth muscle. *Am J Physiol Cell Physiol* 281: C579–C584, 2001
 10. Garg P, Martin CF, Elms SC, Gordon FJ, Wall SM, Garland CJ, Sutliff RL, O'Neill WC: Effect of the Na-K-2Cl cotransporter NKCC1 on systemic blood pressure and smooth muscle tone. *Am J Physiol Heart Circ Physiol* 292: H2100–H2105, 2007
 11. Chiga M, Rai T, Yang SS, Ohta A, Takizawa T, Sasaki S, Uchida S: Dietary salt regulates the phosphorylation of OSR1/SPAK kinases and the sodium chloride cotransporter through aldosterone. *Kidney Int* 74: 1403–1409, 2008
 12. Sohara E, Rai T, Yang SS, Ohta A, Naito S, Chiga M, Nomura N, Lin SH, Vandewalle A, Ohta E, Sasaki S, Uchida S: Acute insulin stimulation induces phosphorylation of the Na-Cl cotransporter in cultured distal mpkDCT cells and mouse kidney. *PLoS ONE* 6: e24277, 2011
 13. Nishida H, Sohara E, Nomura N, Chiga M, Alessi DR, Rai T, Sasaki S, Uchida S: Phosphatidylinositol 3-kinase/Akt signaling pathway activates the WNK-OSR1/SPAK-NCC phosphorylation cascade in hyperinsulinemic db/db mice. *Hypertension* 60: 981–990, 2012
 14. Talati G, Ohta A, Rai T, Sohara E, Naito S, Vandewalle A, Sasaki S, Uchida S: Effect of angiotensin II on the WNK-OSR1/SPAK-NCC phosphorylation cascade in cultured mpkDCT cells and in vivo mouse kidney. *Biochem Biophys Res Commun* 393: 844–848, 2010
 15. Castañeda-Bueno M, Cervantes-Pérez LG, Vázquez N, Uribe N, Kantesaria S, Morla L, Bobadilla NA, Doucet A, Alessi DR, Gamba G: Activation of the renal Na+:Cl- cotransporter by angiotensin II is a WNK4-dependent process. *Proc Natl Acad Sci U S A* 109: 7929–7934, 2012
 16. Chiga M, Rafiqi FH, Alessi DR, Sohara E, Ohta A, Rai T, Sasaki S, Uchida S: Phenotypes of pseudohypoaldosteronism type II caused by the WNK4 D561A missense mutation are dependent on the WNK-OSR1/SPAK kinase cascade. *J Cell Sci* 124: 1391–1395, 2011
 17. Yang SS, Lo YF, Wu CC, Lin SW, Yeh CJ, Chu P, Sytwu HK, Uchida S, Sasaki S, Lin SH: SPAK-knockout mice manifest Gitelman syndrome and impaired vasoconstriction. *J Am Soc Nephrol* 21: 1868–1877, 2010
 18. Filippi BM, de los Heros P, Mehellou Y, Navratilova I, Gourlay R, Deak M, Plater L, Toth R, Zeqiraj E, Alessi DR: MO25 is a master regulator of SPAK/OSR1 and MST3/MST4/YSK1 protein kinases. *EMBO J* 30: 1730–1741, 2011
 19. Vitari AC, Deak M, Morrice NA, Alessi DR: The WNK1 and WNK4 protein kinases that are mutated in Gordon's hypertension syndrome phosphorylate and activate SPAK and OSR1 protein kinases. *Biochem J* 391: 17–24, 2005
 20. Zagórska A, Pozo-Guisado E, Boudeau J, Vitari AC, Rafiqi FH, Thastrup J, Deak M, Campbell DG, Morrice NA, Prescott AR, Alessi DR: Regulation of activity and localization of the WNK1 protein kinase by hyperosmotic stress. *J Cell Biol* 176: 89–100, 2007
 21. Karaman MW, Herrgard S, Treiber DK, Gallant P, Atteridge CE, Campbell BT, Chan KW, Ciceri P, Davis MI, Edeen PT, Faraoni R, Floyd M, Hunt JP, Lockhart DJ, Milanov ZV, Morrison MJ, Pallares G, Patel HK, Pritchard S, Wodicka LM, Zarrinkar PP: A quantitative analysis of kinase inhibitor selectivity. *Nat Biotechnol* 26: 127–132, 2008
 22. Gagnon KB, England R, Delpire E: Characterization of SPAK and OSR1, regulatory kinases of the Na-K-2Cl cotransporter. *Mol Cell Biol* 26: 689–698, 2006
 23. Butini S, Gemma S, Brindisi M, Borrelli G, Lossani A, Ponte AM, Torti A, Maga G, Marinelli L, La Pietra V, Fiorini I, Lamponi S, Campiani G, Zisterer DM, Nathwani SM, Sartini S, La Motta C, Da Settimo F, Novellino E, Focher F: Non-nucleoside inhibitors of human adenosine kinase: Synthesis, molecular modeling, and biological studies. *J Med Chem* 54: 1401–1420, 2011
 24. Koltsova SV, Kotelevtsev SV, Tremblay J, Hamet P, Orlov SN: Excitation-contraction coupling in resistance mesenteric arteries: Evidence for NKCC1-mediated pathway. *Biochem Biophys Res Commun* 379: 1080–1083, 2009
 25. Naito S, Ohta A, Sohara E, Ohta E, Rai T, Sasaki S, Uchida S: Regulation of WNK1 kinase by extracellular potassium. *Clin Exp Nephrol* 15: 195–202, 2011
 26. Mori T, Kikuchi E, Watanabe Y, Fujii S, Ishigami-Yuasa M, Kagechika H, Sohara E, Rai T, Sasaki S, Uchida S: Chemical library screening for WNK signalling inhibitors using fluorescence correlation spectroscopy. *Biochem J* 455: 339–345, 2013
 27. Lin SH, Yu IS, Jiang ST, Lin SW, Chu P, Chen A, Sytwu HK, Sohara E, Uchida S, Sasaki S, Yang SS: Impaired phosphorylation of Na(+)-K (+)-2Cl(-) cotransporter by oxidative stress-responsive kinase-1 deficiency manifests hypotension and Bartter-like syndrome. *Proc Natl Acad Sci U S A* 108: 17538–17543, 2011
 28. Uchida S: Pathophysiological roles of WNK kinases in the kidney. *Pflugers Arch* 460: 695–702, 2010
 29. Kahle KT, Rinehart J, Giebisch G, Gamba G, Hebert SC, Lifton RP: A novel protein kinase signaling pathway essential for blood pressure regulation in humans. *Trends Endocrinol Metab* 19: 91–95, 2008
 30. Richardson C, Alessi DR: The regulation of salt transport and blood pressure by the WNK-SPAK/OSR1 signalling pathway. *J Cell Sci* 121: 3293–3304, 2008
 31. Ashburn TT, Thor KB: Drug repositioning: Identifying and developing new uses for existing drugs. *Nat Rev Drug Discov* 3: 673–683, 2004
 32. Garuti L, Roberti M, Bottegoni G: Non-ATP competitive protein kinase inhibitors. *Curr Med Chem* 17: 2804–2821, 2010
 33. Pedersen SF, O'Donnell ME, Anderson SE, Cala PM: Physiology and pathophysiology of Na+/H+ exchange and Na+ -K+ -2Cl- cotransport in the heart, brain, and blood. *Am J Physiol Regul Integr Comp Physiol* 291: R1–R25, 2006
 34. Bers DM, Barry WH, Despa S: Intracellular Na+ regulation in cardiac myocytes. *Cardiovasc Res* 57: 897–912, 2003
 35. Ohno M, Uchida K, Ohashi T, Nitta K, Ohta A, Chiga M, Sasaki S, Uchida S: Immunolocalization of WNK4 in mouse kidney. *Histochem Cell Biol* 136: 25–35, 2011
 36. Richardson C, Sakamoto K, de los Heros P, Deak M, Campbell DG, Prescott AR, Alessi DR: Regulation of the NKCC2 ion cotransporter by SPAK-OSR1-dependent and -independent pathways. *J Cell Sci* 124: 789–800, 2011
 37. Mutig K, Paliège A, Kahl T, Jöns T, Müller-Esterl W, Bachmann S: Vasopressin V2 receptor expression along rat, mouse, and human renal epithelia with focus on TAL. *Am J Physiol Renal Physiol* 293: F1166–F1177, 2007
 38. Diepens RJ, den Dekker E, Bens M, Weidema AF, Vandewalle A, Bindels RJ, Hoenderop JG: Characterization of a murine renal distal convoluted tubule cell line for the study of transcellular calcium transport. *Am J Physiol Renal Physiol* 286: F483–F489, 2004
 39. Susa K, Kita S, Iwamoto T, Yang SS, Lin SH, Ohta A, Sohara E, Rai T, Sasaki S, Alessi DR, Uchida S: Effect of heterozygous deletion of WNK1 on the WNK-OSR1/ SPAK-NCC/NKCC1/NKCC2 signal cascade in the kidney and blood vessels. *Clin Exp Nephrol* 16: 530–538, 2012

This article contains supplemental material online at <http://jasn.asnjournals.org/lookup/suppl/doi:10.1681/ASN.2014060560/-DCSupplemental>.

Kelch-Like Protein 2 Mediates Angiotensin II–With No Lysine 3 Signaling in the Regulation of Vascular Tonus

Moko Zeniya, Nobuhisa Morimoto, Daiei Takahashi, Yutaro Mori, Takayasu Mori, Fumiaki Ando, Yuya Araki, Yuki Yoshizaki, Yuichi Inoue, Kiyoshi Isobe, Naohiro Nomura, Katsuyuki Oi, Hidenori Nishida, Sei Sasaki, Eisei Sohara, Tatemitsu Rai, and Shinichi Uchida

Department of Nephrology, Graduate School of Medical and Dental Sciences, Tokyo Medical and Dental University, Tokyo, Japan

ABSTRACT

Recently, the kelch-like protein 3 (KLHL3)–Cullin3 complex was identified as an E3 ubiquitin ligase for with no lysine (WNK) kinases, and the impaired ubiquitination of WNK4 causes pseudohypoaldosteronism type II (PHAII), a hereditary hypertensive disease. However, the involvement of WNK kinase regulation by ubiquitination in situations other than PHAII has not been identified. Previously, we identified the WNK3–STE20/SPS1-related proline/alanine-rich kinase–Na/K/Cl cotransporter isoform 1 phosphorylation cascade in vascular smooth muscle cells and found that it constitutes an important mechanism of vascular constriction by angiotensin II (AngII). In this study, we investigated the involvement of KLHL proteins in AngII-induced WNK3 activation of vascular smooth muscle cells. In the mouse aorta and mouse vascular smooth muscle (MOVAS) cells, KLHL3 was not expressed, but KLHL2, the closest homolog of KLHL3, was expressed. Salt depletion and acute infusion of AngII decreased KLHL2 and increased WNK3 levels in the mouse aorta. Notably, the AngII-induced changes in KLHL2 and WNK3 expression occurred within minutes in MOVAS cells. Results of KLHL2 overexpression and knockdown experiments in MOVAS cells confirmed that KLHL2 is the major regulator of WNK3 protein abundance. The AngII-induced decrease in KLHL2 was not caused by decreased transcription but increased autophagy-mediated degradation. Furthermore, knockdown of sequestosome 1/p62 prevented the decrease in KLHL2, suggesting that the mechanism of KLHL2 autophagy could be selective autophagy mediated by sequestosome 1/p62. Thus, we identified a novel component of signal transduction in AngII-induced vascular contraction that could be a promising drug target.

J Am Soc Nephrol 26: ●●●–●●●, 2015. doi: 10.1681/ASN.2014070639

Recently, the kelch-like protein 3 (KLHL3) and Cullin3 (Cul3) were identified as the genes responsible for a hereditary hypertensive disease—pseudohypoaldosteronism type II (PHAII).¹ Because the with no lysine (WNK) kinases (WNK1 and WNK4) had already been identified as the responsible genes for PHAII and the KLHL proteins were known to serve as substrate adaptors of Cul3-based E3 ubiquitin ligase,^{1–3} we speculated and recently showed that KLHL3 functions as an E3 ligase with Cul3 for WNK4 and that the impaired ubiquitination of WNK4 and its subsequent increase within the cell stimulates the downstream OSR1/STE20/SPS1-related proline/alanine-rich kinase (SPAK)–NaCl cotransporter signaling and causes PHAII.⁴ In addition

to WNK4, WNK1 and other WNK kinases (WNK2 and WNK3) have been identified as substrates of KLHL3–Cul3 E3 ligase, because KLHL3 can bind to all WNKs in a highly conserved domain (acidic domain).⁵ Furthermore, we recently reported that KLHL2 possesses a kelch repeat domain (WNK binding domain) highly similar to that of KLHL3 and that

Received July 2, 2014. Accepted October 21, 2014.

Published online ahead of print. Publication date available at www.jasn.org.

Correspondence: Prof. Shinichi Uchida, 1-5-45 Yushima, Bunkyo, Tokyo 113-8519, Japan. Email: suchida.kid@tmd.ac.jp

Copyright © 2015 by the American Society of Nephrology